iJRASET
International Journal For Research in Applied Science and Engineering Technology

INTERNATIONAL JOURNAL FOR RESEARCH

IN APPLIED SCIENCE & ENGINEERING TECHNOLOGY

Volume: 11 **Issue:** II **Month of publication:** February 2023

DOI: https://doi.org/10.22214/ijraset.2023.49179

www.ijraset.com

Call: 08813907089 | E-mail ID: ijraset@gmail.com

International Journal for Research in Applied Science & Engineering Technology (IJRASET)
ISSN: 2321-9653; IC Value: 45.98; SJ Impact Factor: 7.538
Volume 11 Issue II Feb 2023- Available at www.ijraset.com

CFD Analysis of Pressure Variation inside Iron-Ore Slurry Pipelines

Sai Swapnesh Mishra[1], Sibajyoti Danapriya Sahoo[2]
[1]*JSW Steel Ltd., Barbil, Odisha, India*
[2]*Deloitte USI, Bengaluru, Karnataka, India*

Abstract: ***Slurries, basically regarded as two – phase (solid – liquid) mixtures of ore and the carrier medium, generally water, are transported through underground pipelines. The rheological properties of the slurry also play an important role in determining the salient parameters of hydraulic transport such as head loss and pressure drop in commercial slurry pipelines. CFD has provided an upper hand in mathematical modelling and flow simulation, as it provides accurate and dependable flow simulation results. This article primarily focuses on determining the pressure drop across the ends of the pipeline, as slurry flows through it, and to establish a graphical depiction of the various simulations made using different set of conditions.***

The pressure drop for R500 radius of curvature of bends was found to be lying between 4.27% to 6.53%, as the bend angles increased from 3° to 18°, while the same was found to be lying between 3.49% to 6.2% for R2500 radius of curvature of bends. The pressure drop for R500 radius of curvature of bends was found to be lying between 4.91% to 8.3%, as the inlet velocity of slurry increased from 0.5 m/s to 3m/s, while the same was found to be lying between 5.05% to 8.63% for R2500 radius of curvature of bends.

The pressure drop for R500 radius of curvature of bends was found to be lying between as the concentration of solids in slurry increased from 30% to 80%, while the same was found to be lying between 4.09% to 7.62% for R2500 radius of curvature of bends. The pressure drop for R500 radius of curvature of bends was found to be lying between 5.15% to 12.91%, as the diameter of cross section of the pipeline increased from 10 inches to 35 inches, while the same was found to be lying between 5.13% to 12.91% for R2500 radius of curvature of bends. Finally, from the results, it was depicted that, optimal/lower values of inlet velocity, angles of bends, concentration of solids in slurry and diameter of cross section of the pipeline, and with higher values of radius of curvature of bends are the most suitable/optimal flow conditions for slurry inside the pipeline.

Keywords: Slurry transportation, Flow simulation, Slurry rheology, Computational fluid dynamics, Pressure drop, Radius of curvature, Bend angles, Inlet Velocity, Solids concentration.

I. INTRODUCTION

The mineral-industry in India plays an important role in the economic growth of the country on account of the huge deposits of minerals like the iron-ore, manganese ore, copper ore, coal, etc. The growth basically addresses to the non-employment issues pertaining to the vast Indian-population, in addition to the production of the invaluable metals extracted from their respective minerals available in nature. Besides the adoption of efficient metal extraction processes, the transport of the lifted raw-minerals from the mines to the extraction sites, in abundance, possess a real problem pertaining to both cost and effectiveness. In fact, the transport of the minerals to the extraction sites in large quantities at low cost is a challenge that invites serious and careful thinking for preparation of mineral-slurry and its transportation through pipe-lines abandoning the age-old process of mineral transport on road or railways. The Indian subcontinent is rich in minerals and hence subjected to everyday mining throughout the whole landscape. The ores which are produced are being transported by various means such as roadways, railways, waterways, and minutely by pipelines which run underground.

The go of the time is to promote the use of slurry pipelines to any other form of locomotion for the ores to become sustainable and preserve a lot of resources. Over the years, conventional transportation techniques of bulk materials, such as mineral ores, proved to be time consuming, non-economic and prone to losses in several possible ways – thus making the transportation process largely inefficient. A better and attractive means of transportation of mineral ores, as it seems to be, was through underground piping networks. And then, slurry transportation came into the picture. Slurries are basically regarded as two – phase (solid – liquid) mixtures of ore and the carrier medium, generally water, and they are transported through underground pipelines. A suspension of crushed iron ore particles in water forms iron ore slurry.

ISSN: 2321-9653; IC Value: 45.98; SJ Impact Factor: 7.538
Volume 11 Issue II Feb 2023- Available at www.ijraset.com

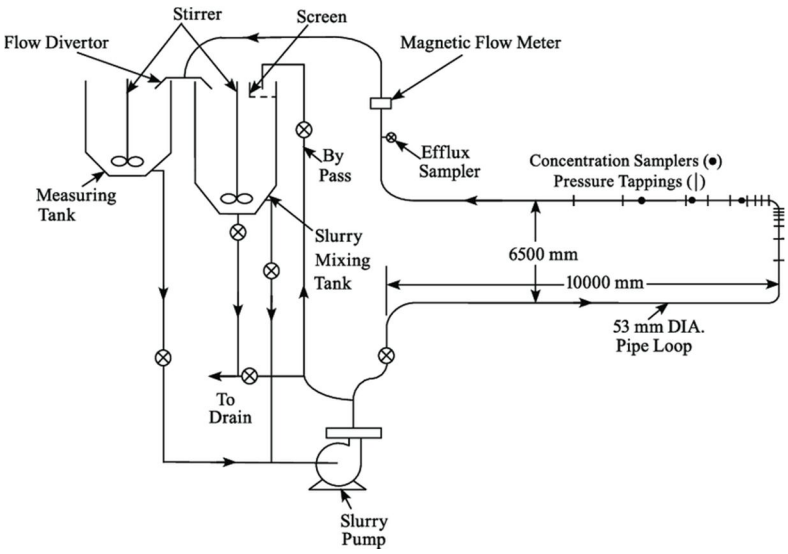

Fig. 1 – Pilot plant test loop for slurry pipeline transportation system [8].

Being beneficial in several ways such as – Transportation of slurry through pipelines is very reliable, it is free from obstacles unlike in road and rail transport; reduction in cost of transportation is very significant; pipelines can be laid through difficult terrains as well as under water; low space required as in case of underground pipelines, the land in which pipeline is laid can still be used for agricultural use; it ensures supply in remote areas where rail or road transportations are not very good; it involves very low energy consumption, easier access for construction and needs very little maintenance; slurry transportation has minimum social impact, shorter route, easier river crossings (without bridging) and minimum unrouted losses; large distance transportation of ultra-fine concentrate will require special wagons, which can be avoided by slurry transportation; slurry can be transported by avoiding the natural calamities like rain, storm, weather change, etc – the process of slurry transportation via pipelines came as a boon to the industries.

But like any other process, the process of slurry preparation and transportation is also laded with several difficulties and disadvantages such as – Slurry pipeline transportation is not flexible, i.e., it can be used only for transportation between two fixed points; pipelines are designed for a fixed capacity and it cannot be increased once it is laid; underground pipelines cannot be easily repaired, and detection of leakage is also difficult; always there is a risk of physical damaging of pipelines which can cause an accident; and like other big linear structures patrolling of pipelines is a huge task, it is very difficult to make security arrangements for pipelines. Researchers have developed several ways to tackle with several such problems, but there are more to take care of [1-8].

One such complication in the pipeline transportation process is pressure drop. Changes in direction of flow caused be Tee fittings, bends, return bends and elbows; losses due to friction, gradual or sudden changes in flow direction or cross section or shape of the pipeline as well as obstructions in the path of flow of slurry are few of the several parameters which lead to abrupt changes in pressure values inside the pipelines. Though an integral part and an important and critical component of any pipeline network, they are of great relevance to the designers of pipelines, and especially those dealing with multiphase (generally, solid-liquid mixtures) fluids. The complexity of flow in bends has been a matter of research for scientists all around the globe, as the bends are quite prone to wear and erosion, and they also cause an additional pressure drop inside the pipeline due to the sudden obstruction to the flow inside the pipeline.

The pressure loss inside slurry pipelines depends strongly upon several parameters such as – flow velocity of slurry, concentration of solid particles in slurry, pipeline diameter/cross section of the pipeline, inclination or bend angles and the radius of curvature of bends. While the determination of pressure drop inside straight pipes is relatively easier, the same for bends is quite difficult, and thus Computational Fluid Dynamics (CFD) comes into the picture. This article primarily focuses to determine the pressure drop and the pressure at other instances of the pipeline, with the help of CFD, by varying the radius of curvature of bends of a pipeline, the inclination angles, initial flow velocity, solid concentration in slurry and diameter of cross section of pipeline by using industrial flow conditions and establish the results [9-15].

ISSN: 2321-9653; IC Value: 45.98; SJ Impact Factor: 7.538
Volume 11 Issue II Feb 2023- Available at www.ijraset.com

Fig. 2 – Bends in slurry pipelines.

II. LITERATURE REVIEW

Tackling with pressure drop inside slurry pipelines has been one of the major cause of worries to researchers since a long time, as pressure losses lead to reduced efficiency of the entire process of slurry transportation.

Doron et. al. (1994) [16] conducted experiments and obtained the flow patterns and pressure drop for the flow of solid-liquid mixtures in pipelines, by giving special emphasis to the range of low mixture flow rates, where a stationary bed is expected. Experimentations and their matching with theoretical data and previously available models were done, and satisfactory agreements were obtained.

Use of transparent pipeline systems revealed that with an increase in flow rates, until its height approaches zero, the stationary deposit does not diminish and rather starts moving as a bulk when its height is several particle diameters. Doron et. al. (1986) [17] investigated the effects of hydraulic transportation of coarse particles in horizontal tubes. For the prediction of flow patterns and pressure drop, they have also presented a physical model. The new data obtained from experimentation, when compared with the proposed model showed satisfactory agreement, and when comparison was done with other proposed correlations, the results thus obtained were also satisfactory.

Singh et. al. [19] used computational fluid dynamics to investigate the flow characteristics of high solid concentration possessing coal-water slurry, using the SST k-ω turbulence model. They used various diameters for a straight pipeline and conducted simulations for a range of slurry inlet velocity. They have stated that with an increase in solid concentration in slurry, flow velocity and particle size of the suspended solids, according to results from numerical simulation, the pressure drop across the ends of the pipeline was found to be increasing non-linearly. Also, the pressure drop was found to be decreasing with an increase in the dimeter of the pipeline carrying coal-water slurry. Similar experiments were also carried out by Kaushal et. al. (2002) [20] and they have proposed an improvised method for the prediction of pressure drop across slurry pipelines.

The study by Chandel et. al. [21], who have conducted the experimentations using a pilot plant test loop to determine the pressure drop across a pipeline carrying fly ash slurry with and without any added additives, showed that pressure drop can be reduced for higher concentration fly ash slurries by additives like soap solution. Wu et. al. [27] used a pilot plant test loop to compare the results of test loop and simulation, for which they had used COMSOL Multiphysics software. They found that the pressure drops for Cemented coal gangue–fly ash (CGF) slurry at varied mix proportions, as determined via simulation and via test loop were in close agreement. They have also demonstrated the combined effect of pipe inner diameter and flow velocity on pressure drop in the pipe loop flow of fresh CGF slurry as well as the effects of slurry volumetric flow rate and pumping pressure, which can thus help in the selection of appropriate pumps capacity.

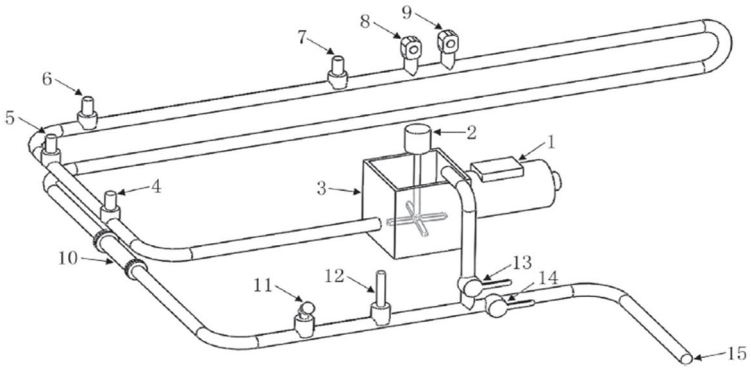

Fig. 3 – Schematic diagram of test loop system used by Wu et. al. [27]

Monterio et. al. [30] reviewed the drop in pressure for flows of ice slurries, also discussing about the variation of pressure drop as a function of concentration of ice, diameter of pipeline and velocity of slurry, with an emphasis on the role of particle diameter in the evaluation of pressure drop. The four rheological models which predict the behavior of ice slurries in pipes – Power, Casson, Bingham and Herschele-Bulkley – were also analyzed. According to them, the data obtained from experimentation agrees with that of rheological models. Li et. al. [31] investigated the influence of the variation in particle sizes on pipeline resistance under varying flow conditions, as, according to them, the existent formulae for determining the pipeline transport resistance of granular materials are based mostly on the experimental data for regularly graded or single-sized particles.

There are several literatures available that determine the frictional pressure loss in slurry pipelines. But, amongst them, several predict the flows of slurry without taking into consideration the deposits in pipelines, though there are several instances, where pipelines were found to be operating with a stationary bed at the bottom of the pipeline, for which models are not largely available. Matoušek [32], in his article has proposed the structure of a predictive model for the frictional pressure drop and the thickness of the stationary bed in a pipe flow of settling slurry at velocities that are too low to maintain all particles in motion. According to various researchers, head losses in rectangular ducts are significantly lower than that in traditional circular pipes. Kaushal et. al. (2003) [34] in their article have conducted experiments with slurries having varied particle sizes of solids, and inlet velocities as well. They have used the traditional circular pipes as well as rectangular ducts for comparative analysis, and have proposed their results, for which they had used rectangular duct with height 50 mm, width 200 mm, and hydraulic diameter 80 mm, as shown in figure 4 below.

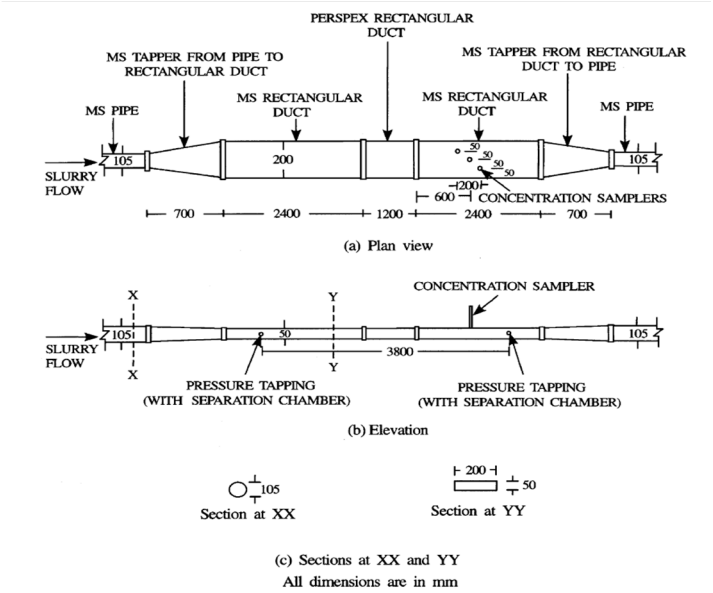

Fig. 4 – Schematic diagram of the rectangular duct used by Kaushal et. al. in their pilot plant test loop [34]

Sudden bends in the pipelines make the internal wall of the pipeline more prone to erosion and wear. Leaks and spills of slurry also abruptly alter the pressure values inside the pipeline, in turn damaging the pipe. Negative pressure, back/slack flow conditions can occur inside pipelines if there are irregularities in pressure. Significant drop in pressure inside the pipelines leads to reduced efficiency and effectiveness of the process. Thus, pressure drops need to be effectively monitored and controlled.

III. MATHEMATICAL MODELS AND EMPIRICAL FORMULAE

While the slurry flows in the pipelines, for any length, the pipelines remain cent percent packed – either with slurry, while the pipelines are operational; or with water, when there is a shutdown of the plant. For iron ore slurry, the solid concentration is maintained at 63-67% and the specific gravity generally remains around 3.6. For better results in transportation, the particle size is kept at 150 microns, while it can also be increased to 212 microns if the profile is smooth. The maximum allowable slope is 12% or 7º, otherwise, there can be chances of losses. Most of the losses in pipelines happen due to the settling of the slurry at the bottom of the pipelines which reduces their efficiency. Hence, an optimal velocity is maintained inside the pipelines throughout. The velocity at which the particles start settling at the bottom is called the critical deposition velocity. The optimal velocity is kept higher than the critical deposition velocity. The general equation for this is given by [22-23,29,33,35] –

$$\text{Operational velocity} = 0.5\text{m/s} + \text{Deposition velocity } (V_c) \quad \text{(i)}$$

A. Governing Equations and Relations

The Eulerian model is used as it is an effective model to tackle the continuity and momentum equation for each phase and coupling between the phases is accomplished through pressure and interexchange coefficients. In Eulerian model, the slurry bend supposed to be comprised of solid (α_s) and liquid (α_f) phases, i.e., $\alpha_s + \alpha_f = 1$. In the present model, granular flow properties are attaining from kinetic theory applications. The solid particles in the slurry flow subjected to the following forces, i.e., Static/Solid pressure gradient ($\nabla P/\nabla P_S$), viscous force ($\nabla.\bar{\bar{\tau}}_f$), where, $\bar{\bar{\tau}}_f$ is the viscous stress tensor for fluid phase, and body forces ($\rho\vec{g}$), where, ρ is the mass density in kg/m^3 and $\vec{g}$ is the acceleration due to gravity in m/s^2, Lift/virtual forces and forces due to phase velocities difference (K_{sl} ($\vec{v}_s$ - $\vec{v}_l$)), where K_{sl} represents the interphase momentum exchange coefficient, and $\vec{v}_s$ and $\vec{v}_l$ are velocities of solid phase and liquid phase respectively. The solid particulates in the fluid domains are assumed to be spherical in shape and by nature, fluidic [18,24,28].

1) The Governing Equations

The equations governing flow of slurry are:

$$\nabla.(\alpha_t \rho_t \vec{v}_t) = 0 \quad \text{(i)}$$

And in this case, *t* can be considered as *s* or *l*.

2) Momentum Equations for Fluid and Solid Phases

For liquid phase:

$$\nabla.(\alpha_l \rho_l \vec{v}_l \vec{v}_l) = -\alpha_l \nabla P + \nabla.(\bar{\bar{\tau}}_l + \bar{\bar{\tau}}_{f,l}) + \alpha_l \rho_l \vec{g} + K_{sl}(\vec{v}_s - \vec{v}_l) + C_{vm}\alpha_s\rho_l(\vec{v}_s.\nabla\vec{v}_s - \vec{v}_l.\nabla\vec{v}_l) + C_L\alpha_s\rho_l(\vec{v}_l - \vec{v}_s)\times(\nabla\times\vec{v}_l) \quad \text{(ii)}$$

For solid phase:

$$\nabla.(\alpha_s \rho_s \vec{v}_s \vec{v}_s) = -\alpha_s \nabla P - \nabla P_s + \nabla.(\bar{\bar{\tau}}_s + \bar{\bar{\tau}}_{f,l}) + \alpha_s \rho_s \vec{g} + K_{ls}(\vec{v}_l - \vec{v}_s) + C_{vm}\alpha_s\rho_l(\vec{v}_l.\nabla\vec{v}_l - \vec{v}_s.\nabla\vec{v}_s) + C_L\alpha_s\rho_l(\vec{v}_s - \vec{v}_l)\times(\nabla\times\vec{v}_l) \quad \text{(iii)}$$

Where, $\bar{\bar{\tau}}_{f,l}$ is the Reynolds stress tensor, whereas, $\bar{\bar{\tau}}_l$ and $\bar{\bar{\tau}}_s$ are the viscous stress tensors for liquid and solid phase respectively, which are given by:

$$\bar{\bar{\tau}}_l = \alpha_l\mu_l(\nabla\vec{v}_l - \nabla\vec{v}_l^{\,fr}) \quad \text{(iv)}$$

$$\bar{\bar{\tau}}_s = \alpha_s\mu_s(\nabla\vec{v}_s - \nabla\vec{v}_s^{\,fr}) + \alpha_s(\lambda_s - \tfrac{2}{3}\mu_s)\,\nabla\vec{v}_s\bar{\bar{I}} \quad \text{(v)}$$

Where, '*fr*' in superscript above the velocity vector represents the transpose, $\bar{\bar{I}}$ represents the identity tensor, and the bulk viscosity of solid, as shown below, is given by λ_s:

$$\lambda_s = \frac{4}{3}\alpha_s\rho_s d_s g_{o,ss}(1+e_{ss})\left(\frac{\Theta_s}{\pi}\right)^{\frac{1}{2}} \quad \text{(vi)}$$

Where, d_s is the diameter of the particles and $g_{o,ss}$ is the radial distribution function which is defined as –

$$G_{o,ss} = \left[1 - \left[\frac{\alpha_s}{\alpha_{s,max}}\right]^{\frac{1}{3}}\right]^{-1} \quad \text{(vii)}$$

Here, $\alpha_{s,max}$ is the static settled concentration, Θ_s is the granular temperature, e_{ss} is the restitution of coefficient and μ_l is the shear viscosity of liquid. Solid shear viscosity, μ_s is represented as –

$$\mu_s = \mu_{s,col} + \mu_{s,kin} + \mu_{s,Ir} \quad \text{(viii)}$$

Where, $\mu_{s,col}$, $\mu_{s,kin}$, and $\mu_{s,Ir}$ are the collisional, kinetic and frictional viscosities respectively, which are given as:

$$\mu_{s,col} = \frac{4}{5}\alpha_s \rho_s d_s g_{o,ss}(1+e_{ss})\left(\frac{\Theta_s}{\pi}\right)^{\frac{1}{2}} \quad \text{(ix)}$$

$$\mu_{s,Ir} = \frac{P_s \sin\varphi}{2\sqrt{I_{2D}}} \quad \text{(x)}$$

$$\mu_{s,kin} = \left[\frac{\alpha_s d_s \rho_s \sqrt{\Theta_s \pi}}{6(3-e_{ss})}[1+0.4(1+e_{ss})(3e_{ss}-1)\alpha_s g_{o,ss}\right] \quad \text{(xi)}$$

I_{2D} is another invariant of the deviatory strain rate tensor defined for solid phase, φ is the internal friction angle and P_s does represent the solid pressure, as shown below –

$$P_s = \alpha_s \rho_s \Theta_s + 2\rho_s(1+e_{ss})\alpha_s^2 g_{0,ss}\Theta_s \quad \text{(xii)}$$

K_{sl} represents the inter-phase momentum exchange coefficient, defined as –

$$K_{sl} = K_{ls} = \frac{3}{4}\frac{\alpha_s \alpha_l \rho_l}{V_{r,s}^2 d_s} C_D\left(\frac{\mathrm{Re}_s}{V_{r,s}}\right)\left|\vec{V_s} - \vec{V_l}\right| \quad \text{(xiii)}$$

C_D represents the drag coefficient defined by:

$$C_D = \left(0.63 + 4.8\left(\frac{\mathrm{Re}_s}{V_{r,s}}\right)^{\frac{-1}{2}}\right)^2 \quad \text{(xiv)}$$

Re_f is the relative Reynolds Number for the liquid and solid phase and is defined as:

$$\mathrm{Re}_f = \frac{\rho_l d_s \left|\vec{V_s} - \vec{V_l}\right|}{\mu_l} \quad \text{(xv)}$$

$V_{r,s}$ represents the terminal velocity of the solid phase.

B. Different flow Parameters and Relations

Some of the factors on which the slurry flow depends are – forces at different segments in the pipe, friction, density, heat transfer and many more. The much important ones will be discussed in details in the upcoming sections.

The force acting upon a fluid due to pressure difference between two sections of pipe is given as –

$$F = \frac{\pi}{4}D^2(P_1 - P_2) \quad \text{(xvi)}$$

While, the force acting on the fluid at the pipe wall is –

$$F = (-\tau_W \times Area) = -\tau_W \pi D L \quad \text{(xvii)}$$

The negative sign in the latter equation suggests that the force is opposite to the direction to the flow. Now, both the above forces should add up to zero to maintain equilibrium. Hence,

$$\frac{\pi}{4}D^2(P_1 - P_2) - \tau_W \pi D L = 0$$

$$\Longrightarrow \tau_W = \frac{D(P_1 - P_2)}{4L} \quad \text{(xviii)}$$

The Fanning's frictional factor, f, which is the ratio of the frictional forces to the inertial forces is given by –

$$f = \frac{\tau_W}{\frac{\rho U^2}{2}} = \frac{\frac{(\Delta P)D}{4L}}{\frac{\rho U^2}{2}} \quad \text{(xix)}$$

The formula for density of a suspension is –

$$\rho_m = \frac{100}{\frac{C_w}{\rho_s} + \frac{100 - C_w}{\rho_l}} \quad \text{(xx)}$$

The relationship between solid's specific gravity (ρ_s), volume percent solids (C_v), specific gravity of the suspending medium (ρ_m), and weight percent concentration of solid (C_w) is given by –

$$C_v = \frac{100\, {C_w}/{\rho_S}}{\frac{C_w}{\rho_S} + \frac{100 - C_w}{\rho_S}} = \frac{C_w \rho_M}{\rho_S} \quad \text{(xxi)}$$

or,

$$C_w = \frac{C_v \rho_S}{C_v \rho_S + (100 - C_v)} = \frac{C_v \rho_S}{\rho_M} \quad \text{(xxii)}$$

C. Relationship Between Critical Deposition velocity and pipeline Diameter

The critical deposition velocity has always been a major challenge in the slurry transportation process. Responsible for decreased efficiency and sometimes chokes also, this hurdle has only one solution – to maintain an optimized velocity inside the pipelines so that settling doesn't take place. It is quite important to establish a relationship between critical deposition velocity and diameter of the pipe so that the desired value of the optimal velocity can be found out and applied when needed, thus solving the problem of settling of heavier particles at the bottom of the pipe by avoiding that scenario altogether.

1) The Durand Correlation (1952)

Durand in 1952 proposed an equation for uniformly sized particles which related critical deposition velocity to the pipeline diameter. The equation is as follows –

$$V_D = F_L \left[2gD\left(\frac{\rho_s - \rho_l}{\rho_l}\right)\right]^{1/2} \quad \text{(xxiii)}$$

Where F_L is a constant and varies from system to system as it is a function of solid concentration and particle size. Wicks modified the above equation for dilute suspensions in wholly turbulent flow and proposed the below equation by taking the particle diameter as a variable –

$$V_D = F_L \left(\frac{d}{D}\right)^{1/6} \left[2gD\left(\frac{\rho_s - \rho_l}{\rho_l}\right)\right]^{1/2} \quad \text{(xxiv)}$$

2) The Gillies and Shook Model (2000)

Gillies and Shook modified the Durand – Condolis equation, and in 2000, proposed an equation which suggested that the Archimedes Number should be the principal independent variable in the relation. The dependent variable in this correlation is the Froude number, which is used to calculate the deposition velocity. The ratio of gravitational forces acting on the particle, corrected for buoyancy, to viscous forces acting on the particle is known as the Archimedes Number. Mathematically,

$$Ar = \frac{4}{3}\frac{g d^3 (S - 1)\rho_f^2}{\mu_f^2} \quad \text{(xxv)}$$

Now, the Froude Number, which is defined as the ratio of inertial forces in the fluid flow to the gravitational forces the particle must overcome to stay suspended in the flow, is related to the Archimedes number by the below relations –

$$For\ 540 < Ar;\ Fr = 1.78Ar^{-0.019}$$
$$For\ 160 < Ar < 540;\ Fr = 1.19Ar^{0.045} \quad \text{(xxvi)}$$
$$For\ 80 < Ar < 160;\ Fr = 0.197Ar^{0.4}$$

Mathematically, Froude number is given as –

$$Fr = \frac{V_c}{\sqrt{gD(S-1)}} \quad \text{(xxvii)}$$
$$\Rightarrow V_c = Fr\sqrt{gD(S-1)}$$

Thus, this is the modified relation between critical deposition velocity of slurry and the diameter of the pipeline. Using these relations, the settling velocity can be found out and the value for optimal velocity can be decided. The reason why an optimized velocity needs to be maintained in the pipeline is that – while a reduced velocity will lead to the formation of bed deposition layer which in turn reduces the carrying capability of pipelines, an increased velocity will lead to the internal corrosion of the pipes which in long run affects the longevity of the pipelines severely.

D. Viscosity Relations

The equations of viscosity and other relations provided by D.G. Thomas in 1965 prove to be very useful in relating several parameters that largely affect the slurry transportation process. The equations for Newtonian slurry are –

$$\text{Volume concentration } (C_v) = \frac{1}{\left[1+\left(\frac{100-C_w}{C_w}\right)\times\frac{\rho_S}{\rho_l}\right]} \quad \text{(xxviii)}$$

$$\text{Ratio of viscosities } \left(\frac{\mu_p}{\mu_f}\right) = [1 + (2.5 \times C_v) + (10.05 \times C_v^2) + (0.00273 \times (e^{16.6\times C_v}))] \quad \text{(xxix)}$$

$$\text{Pulp dynamic viscosity } (\mu_p) = \left(\frac{\mu_p}{\mu_f}\right) \times \mu_w \quad \text{(xxx)}$$

$$\text{Pulp density } (\rho_p) = \frac{\rho_l \times S_S}{C_w+((1-C_w)\times S_S)} \quad \text{(xxxi)}$$

Using these established mathematical models and equations, the desired theoretical aspects of pipeline flow can be determined and used during the design and construction of upcoming/planned pipeline projects

IV. CFD AND FLOW SIMULATION

The flow of slurry in pipelines can be classified into two broad categories, among several others, as – homogeneous flow and heterogeneous flow.

1) *Homogeneous Flow:* In this type of flow, solids are evenly distributed throughout the liquid medium. This condition is encountered in slurries of high concentrations and fine particle sizes. Here, a sharp increase in viscosity and minor particle inertia effects can be observed while the rheology of the slurry is non-Newtonian.
2) *Heterogeneous Flow:* Solids are not evenly distributed in this case. Inertial effects are significant and only a small rise in viscosity can be witnessed. The concentration of solids remains low and the size of the particles is larger.

Used increasingly in modern times, computational fluid dynamics (CFD) has opened the doors of vast ways of solving problems – via computation and numerical simulations. It has wide field of applications, ranging from heat exchangers to aeronautics, from microchips to transportation techniques making it quite efficient and reliable. The excessive expensive and time-consuming method of physical testing and experimentation makes it impractical in some cases, and that's where CFD comes to the rescue. Used increasingly in cases of multiphase flow, CFD, approach has the advantage that 3-D solid-liquid flow problems under a wide range of flow conditions and flow regimes can be rapidly evaluated, which is otherwise experimentally impossible. Several software such as SolidWorks, Ansys Fluent and COMSOL Multiphysics help in solving real life problems via CFD. Generally, the Eulerian model, in CFD modelling, is used for the prediction of pressure drop and solid concentration distribution, and the results shown by this model were found to be quite accurate and close to the experimental results, as stated by several researchers, who have worked on the analysis of effected on flow and rheological behaviour by CFD modelling. While the Eulerian model solves momentum and continuity equations for each phase, the Navier-Stokes equations are based on the conservation of mass, momentum and energy.
Flow simulation of multiphase flows are quite complex by nature.

ISSN: 2321-9653; IC Value: 45.98; SJ Impact Factor: 7.538
Volume 11 Issue II Feb 2023- Available at www.ijraset.com

The reasons for this being – the existence of various types of sloe (solid-liquid, solid-gas, liquid-gas, etc.) and the existence of several flow regimes such as – homogeneous flow, heterogeneous flow, laminar flow, turbulent flow, etc. Another reason for the complexity of CFD modelling and simulation is the involvement of several numerical parameters, mathematical equations, empirical models, & governing laws and boundary conditions – the numerical and laws of which are extremely complex. Lack of experimental validation to the simulation results. Multiphase modelling also brings along with it, effects such as solid–liquid interaction, drag, break-up, interface dynamics and coalescence, making matters a bit more complex. Almost all CFD codes apply extensions of single-phase solving procedures, leading to diffusive or unstable solutions, and require very short time-steps. Considering these apparent limitations in CFD modelling and simulation, the present work has been undertaken to systematically develop a CFD based model to predict the pressure drop in slurry pipeline [25-26,36-45].

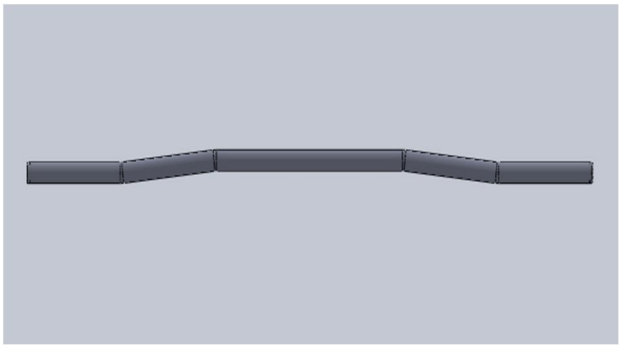

Fig. 5 – Model of the pipeline used for simulation

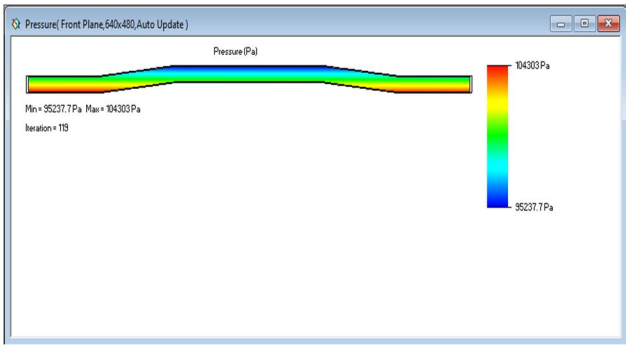

Fig. 6 – CFD analysis of slurry flow inside the pipeline

In this simulation work, iron ore slurry has been considered for flow inside pipelines, having a constant and circular cross section. The pipeline material is made up of high-density polyethylene (HDPE) for its properties gives better flow results as compared to other pipeline materials.

The density of slurry can vary from 2500-3600 kg/m^3 depending upon the grade of iron ore. The chemical composition of iron ore, which varies from mine to mine, affects the overall density of slurry thus formed, with water as the career medium. 5 sets of radiuses of curvatures of bends were considered during simulation – R500, R1000, R1500, R2000, R2500 – and a total of 4 sets of conditions, namely – the angle of bends of the pipeline, concentration of the solids in slurry, inlet velocity and the area of the cross section of the pipeline – were varied in this project for each of the radii of curvature and pressure drop across the ends of the pipeline, pressure values at the various bends of the pipeline along with the maximum and minimum pressure inside the pipe were observed via simulation.

The various sets of conditions used were – Angles of bents in the pipeline (3º, 6º, 9º, 12º, & 15º), areas of cross section of the pipeline (10in, 15in, 20in, 25in, 30in, & 35in), inlet velocity (0.5m/s, 1.0m/s, 1.5m/s, 2.0m/s, 2.5m/s, & 3.0m/s) and concentration of solids in slurry by weight (30%, 40%, 50%, 60%, 70% & 80%). The various sets of parameters which were kept constant, while varying any of the other parameters were – inlet velocity:1.5m/s, angle of bent:6º, concentration of solids:67%, and area of cross section of the pipe:15 inch. The pipeline consists of 4 bends. The multiphase model with a standard k-ε turbulence model and based on the Eulerian-Eulerian approach along with mixture properties was used in this process.

V. RESULTS AND DISCUSSIONS

After obtaining the desired results through CFD based flow simulation, and tabulating them, the graphs for various variations were plotted.

A. For Radius of Curvature of Bends – R500

1) Variation of Pressure drop with Varying bend Angles of the Pipeline

The variations of the angles of bends of the pipeline were done by keeping the area of cross section/outer diameter of the pipeline constant at 15 inches, and inlet velocity of slurry constant at 1.5 m/s. The inner diameter of the pipeline in all the cases was also maintained at 14.5 inches. The bend angles were varied as follows - 3°, 6°, 9°, 12°, 15°, and 18°, respectively. The radius of curvature of pipeline bend was also kept constant at R500. The results thus obtained are shown in Table 1 below, and also plotted in graphs.

Table 1 – Variation of pressure inside the pipeline with an increase in bend angles

Bend Angles (in º)	Pressure values in the pipeline (in Pa)								
	Maximum Pressure	Minimum Pressure	Pressure at the Inlet	Pressure at the Outlet	Pressure Drop	Pressure at Bend 1	Pressure at Bend 2	Pressure at Bend 3	Pressure at Bend 4
3	105322	97293.7	103831.88	99393.67	4438.21	101101.83	99896.47	100187.93	101395.34
6	105368	95554.6	103871.96	99243.66	4628.3	101394.53	98667.81	98166.71	101646.25
9	105557	93861.4	105123.52	99192.07	5931.45	102106.59	97250.16	96730.17	101668.77
12	105675	92150.2	105317.98	99113.92	6204.06	102147.12	95234.27	95404.94	102112.08
15	105794	90468.6	105448.85	98733.23	6715.62	102306.55	94096.91	93549.35	102282.65
18	105895	88821.4	105612.41	98711.49	6900.92	102391.19	92024.35	91857.16	102306.12

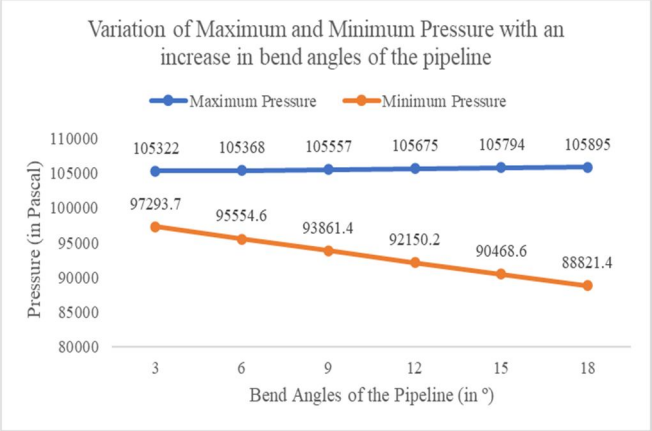

Fig. 7 – Variation of maximum and minimum pressure inside the pipe with increase in bend angles of the pipe

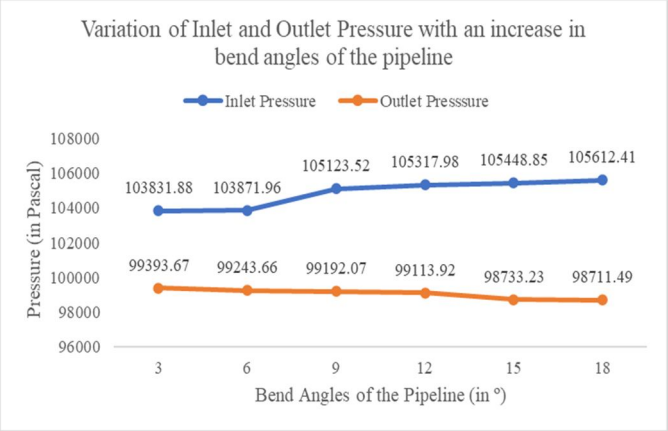

Fig. 8 – Variation of inlet and outlet pressure inside the pipeline with an increase in the bend angles of the pipe

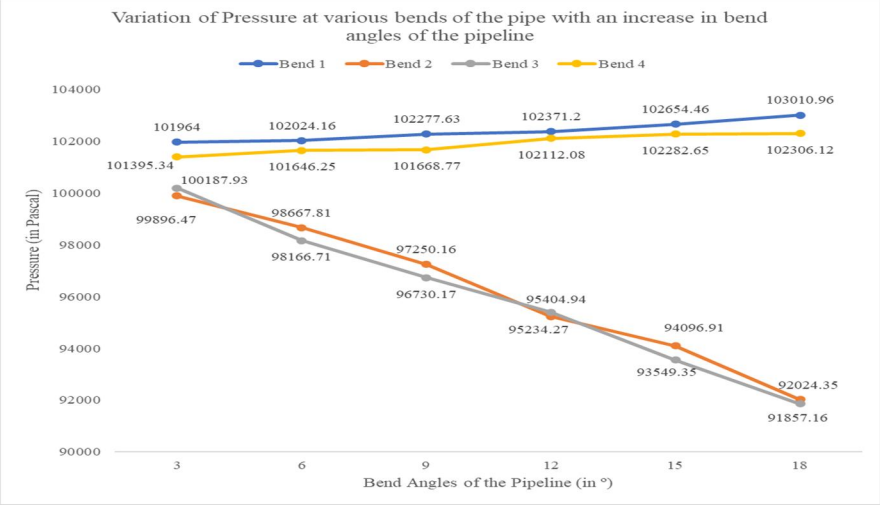

Fig. 9 – Variation pressure at various bends inside the pipeline with an increase in the bend angles of the pipe

The graphs represented in fig. 7, fig. 8 and fig. 9 indicate the plot of maximum and minimum pressure inside the pipeline vs. bend angles of the pipe system, pressure at the inlet and outlet of the pipe vs. bend angles of the pipe system, and the pressure at various bents of the pipeline with respect to the bend angles, respectively, which were plotted taking into consideration the values obtained from table 1. The observations made are – with an increase in angle of bend of the pipeline system from 3º to 18º, the maximum pressure increased marginally from 105322 Pa to 105895 Pa, and the minimum pressure dropped substantially from 97293.7 Pa to 88821.4 Pa. While the pressure at the inlet also somewhat noticeably increased, from 103831.88 Pa to 105612.41 Pa, the pressure at the outlet dropped from 99393.67 Pa to 98711.49 Pa. The value of pressure drop was found to be ranging between 5120.39 Pa and 6218.74 Pa, or 4.27% to 6.53%. While the pressure at bends 1 and 4 of the pipeline system were found to be increasing, the same in bends 2 and 3 were found to be decreasing with an increase in the angles of bend of the pipeline.

2) Variation of Pressure Drop with Varying Inlet Velocity of Slurry

The variations of the inlet velocity of slurry were done by keeping the area of cross section/outer diameter of the pipeline constant at 15 inches, and bend angles at 6º. The inner diameter of the pipeline in all the cases was also maintained at 14.5 inches. The inlet velocities were varied as follows – 0.5 m/s, 1.0 m/s, 1.5 m/s, 2.0 m/s, 2.5 m/s, and 3.0 m/s respectively. The radius of curvature of pipeline bend was also kept constant at R500. The results thus obtained are shown in Table 2 below, and also plotted in graphs.

Table 2 – Variation of pressure inside the pipeline with an increase in inlet velocity of slurry

Inlet Velocity (in m/s)	Pressure values in the pipeline (in Pa)								
	Maximum Pressure	Minimum Pressure	Pressure at the Inlet	Pressure at the Outlet	Pressure Drop	Pressure at Bend 1	Pressure at Bend 2	Pressure at Bend 3	Pressure at Bend 4
0.5	104303	95237.7	104016.37	98906.78	5109.59	101039.41	98057.38	98215.81	101083.33
1.0	104722	95375.1	104182.82	98948.86	5233.96	101648.21	98154.22	98380.42	101244.49
1.5	105406	95602.5	104913.64	98952.38	5961.26	102619.36	98646.2	98481.95	101342.23
2.0	106335	95907.4	105671.92	98986.74	6685.18	102973.29	98994.77	98770.26	101549.06
2.5	107487	96276.1	106805.58	99043.25	7762.33	104006.83	99795.35	98848.38	101789.34
3.0	108883	96730.6	108023.42	99058.2	8965.22	105323.45	100805.06	99446.94	102190.66

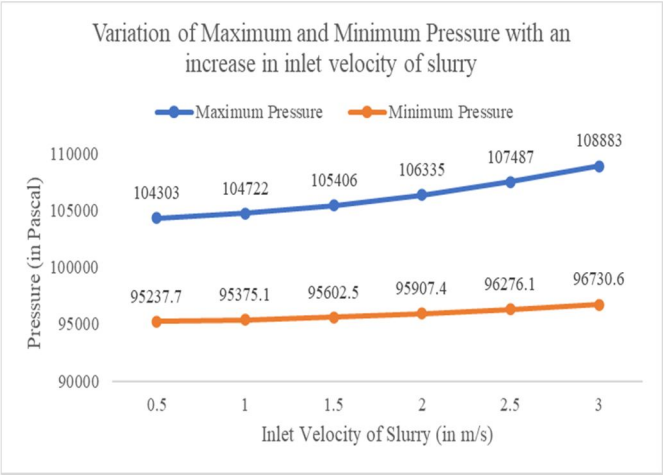

Fig. 10 – Variation of maximum and minimum pressure inside the pipe with increase in inlet velocity of slurry

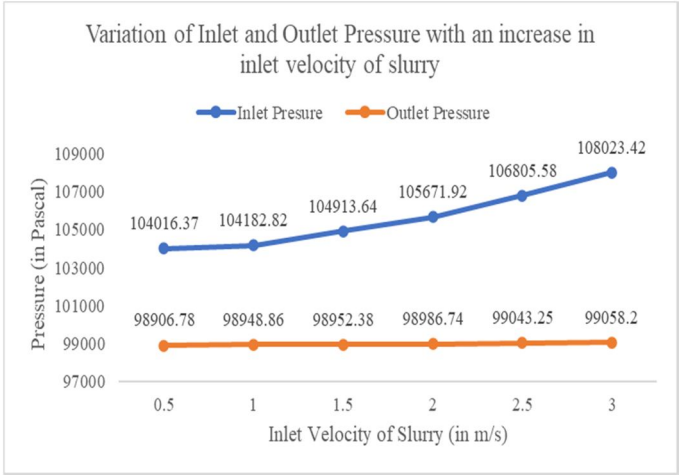

Fig. 11 – Variation of inlet and outlet pressure inside the pipeline with an increase in the inlet velocity of slurry

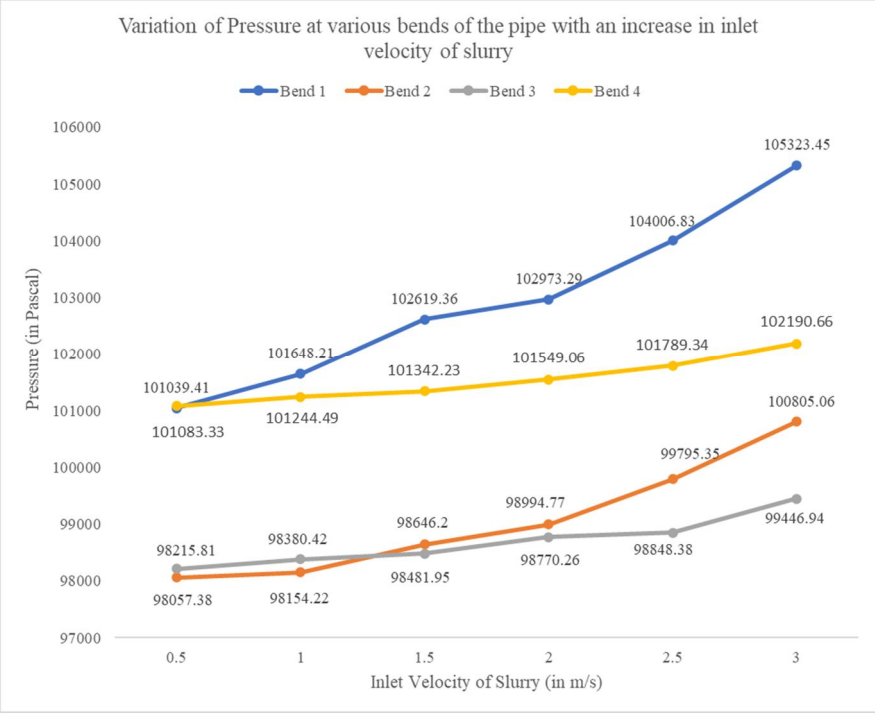

Fig. 12 – Variation pressure at various bends inside the pipeline with an increase in the inlet velocity of slurry

The graphs represented in fig. 10, fig. 11 and fig. 12 indicate the plot of maximum and minimum pressure inside the pipeline vs. inlet velocity of slurry, pressure at the inlet and outlet of the pipe vs. inlet velocity of slurry, and the pressure at various bents of the pipeline with respect to the inlet velocity of slurry, respectively, which were plotted taking into consideration the values obtained from table 2. The observations made are – with an increase in velocity at the inlet of the pipeline system from 0.5 m/s to 3 m/s, the maximum pressure increased substantially from 104303 Pa to 108883 Pa, and the minimum pressure increased minorly from 95237.7 Pa to 96730.6 Pa. Both the pressures at the inlet and the outlet increased during the process, albeit the rise in pressure at the inlet was steep, i.e., from 104016.37 Pa to 108023.42 Pa, as compared to the marginal rise in pressure at the outlet of the pipe, i.e., from 98906.78 Pa to 99058.2 Pa. The value of pressure drop was found to be ranging between 5109.59 Pa and 8965.22 Pa, or 4.91% to 8.3%. The pressure at bends at all the 4 bends were found to be increasing with an increase in the inlet velocity of slurry.

3) Variation of Pressure Drop with Varying Concentration of Solid Particles in Slurry

The variations of the concentration of solids in slurry were done by keeping the area of cross section/outer diameter of the pipeline constant at 15 inches, and inlet velocity of slurry constant at 1.5 m/s. The inner diameter of the pipeline in all the cases was also maintained at 14.5 inches. The concentration of solids in slurry were varied as follows – 30%, 40%, 50%, 60%, 70% and 80% respectively. The radius of curvature of pipeline bend was also kept constant at R500. The results thus obtained are shown in Table 3 below, and also plotted in graphs.

Table 3 – Variation of pressure inside the pipeline with an increase in concentration of solids in slurry

Concentration of solids in slurry (in %)	Pressure values in the pipeline (in Pa)								
	Maximum Pressure	Minimum Pressure	Pressure at the Inlet	Pressure at the Outlet	Pressure Drop	Pressure at Bend 1	Pressure at Bend 2	Pressure at Bend 3	Pressure at Bend 4
30	104074	97187.7	103870.19	99588.97	4281.22	101800.3	99280.91	99023.89	101258.85
40	104318	96823.7	104100.81	99441.92	4658.89	102105.19	99046.08	98999.99	101339.3
50	104633	96443.3	104371.36	99271	5100.36	102140.99	98735.41	98754.67	101422.77
60	105025	95971.2	104780.48	99061.74	5718.74	102217.73	98711.57	98303.9	101501.96
70	105627	95445.2	105396.16	98809.44	6586.72	102401.15	98671.53	98025.66	101517.11
80	106915	94903.3	106658.2	98491.19	8167.01	103174.89	98636.41	97873.18	101540.42

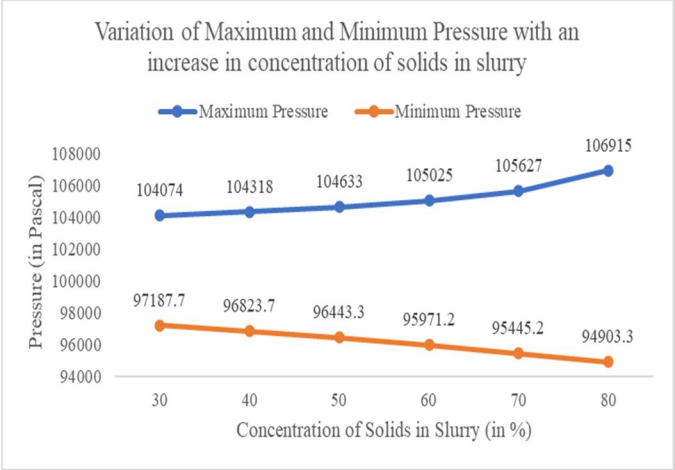

Fig. 13 – Variation of maximum and minimum pressure inside the pipe with increase in concentration of solids in slurry

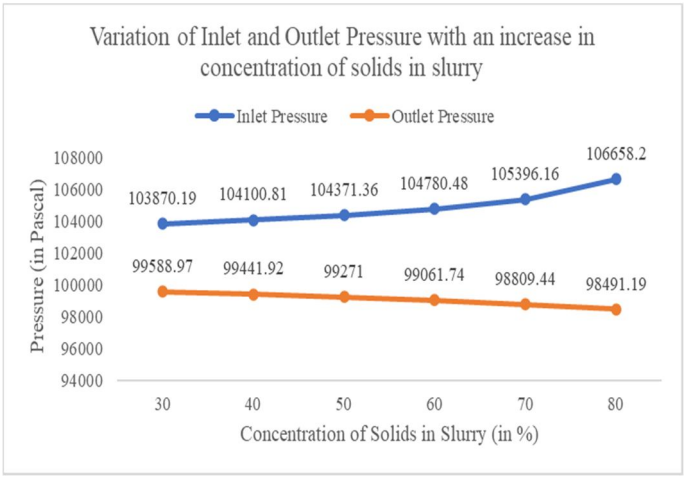

Fig. 14 – Variation of inlet and outlet pressure inside the pipeline with an increase in the concentration of solids in slurry

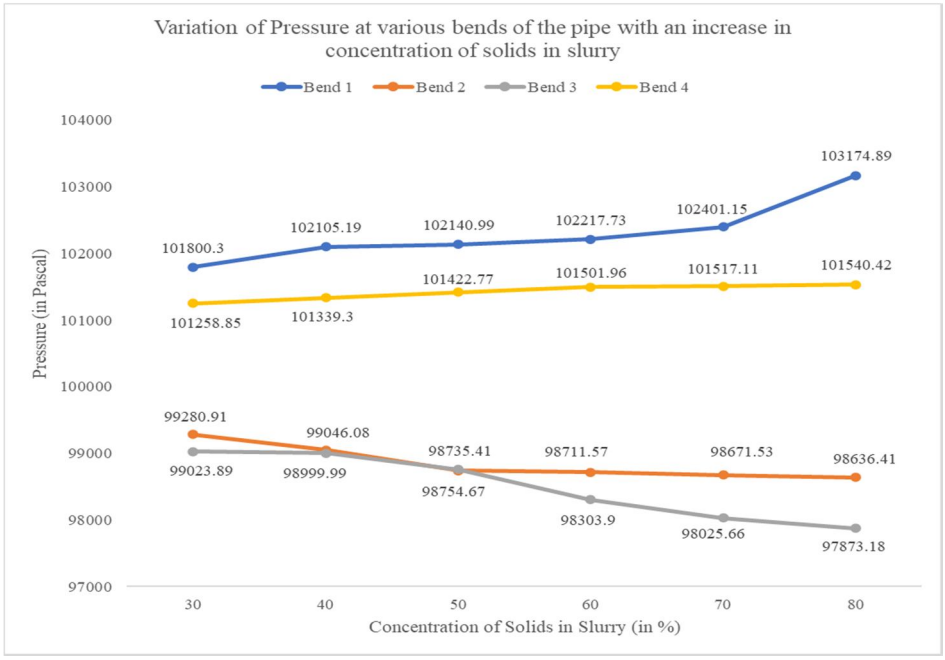

Fig. 15 – Variation pressure at various bends inside the pipeline with an increase in concentration of solids in slurry

The graphs represented in fig. 13, fig. 14 and fig. 15 indicate the plot of maximum and minimum pressure inside the pipeline vs. concentration of solids in slurry, pressure at the inlet and outlet of the pipe vs. concentration of solids in slurry, and the pressure at various bents of the pipeline with respect to the concentration of solids in slurry, respectively, which were plotted taking into consideration the values obtained from table 3. The observations made are – when the concentration of solids in the slurry flowing inside the pipeline was increased from 30% to 80%, the maximum pressure was found to be increasing from 104074 Pa to 106915 Pa, while the minimum pressure inside the pipeline decreased notably from 97187.7 Pa to 94903.3 Pa. Also, while the inlet pressure varied in the same manner as the maximum pressure, slow initially and steeper afterwards, from 103870.19 Pa to 106658.2 Pa, the outlet pressure fell minorly during the process, from 99588.97 Pa to 98491.19 Pa. The value of pressure drop was found to be ranging between 4281.22 Pa and 8167.01 Pa, or 4.12% to 7.65%. While the pressure at bend 1 of the pipeline system were found to be increasing rapidly, the same for bend 4 was found to be rising albeit slowly, while the same in bends 2 and 3 were found to be decreasing, though for bend 2, it decreased slowly and for bend 3 it decreased rapidly with an increase in concentration of solid particles in slurry.

4) Variation Of Pressure Drop With Varying Diameter Of Cross Section Of Pipeline

The variations of the diameter of cross section of the pipeline were done by keeping the bend angles of the pipe constant at 6º, and inlet velocity of slurry constant at 1.5 m/s. The inner diameter of the pipeline in all the cases was also maintained at 0.5 inches less than the outer diameter. The diameter of cross section of the pipeline were varied as follows – 10 inches, 15 inches, 20 inches, 25 inches, 30 inches, 35 inches respectively. The radius of curvature of pipeline bend was also kept constant at R500. The results thus obtained are shown in Table 4 below, and also plotted in graphs.

Table 4 – Variation of pressure inside the pipe with an increase in diameter of cross section of pipe

Diameter of the pipeline (in Inches)	Pressure values in the pipeline (in Pa)								
	Maximum Pressure	Minimum Pressure	Pressure at the Inlet	Pressure at the Outlet	Pressure Drop	Pressure at Bend 1	Pressure at Bend 2	Pressure at Bend 3	Pressure at Bend 4
10	105122	96597.6	105012.44	99597.56	5414.88	101964	99118.35	98163.37	101396.01
15	105546	95356.1	105257.07	98653.45	6603.62	102024.16	98667.24	98335.61	101426.12
20	106340	94184.8	105936.22	97648.19	8288.03	102277.63	98427.66	98409.16	101531.75
25	107280	93052.4	106753.27	96646.56	10106.71	102371.2	98305.37	98445.19	101557.65
30	108264	91924.3	107618.68	95571.55	12047.33	102654.46	98291.23	98677.62	101613.72
35	109278	90832.7	108627.67	94595.9	14031.77	103010.96	97715.64	98715.33	101936.4

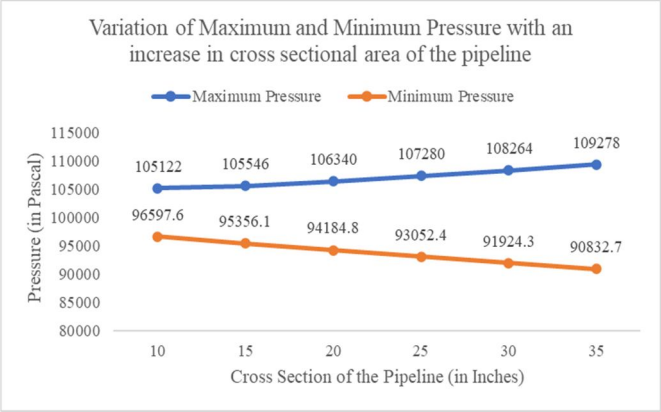

Fig. 16 – Variation of maximum and minimum pressure inside the pipe with increase in diameter of cross section of the pipeline

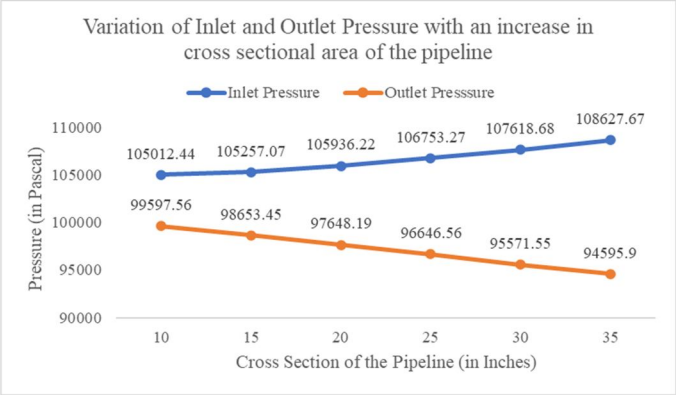

Fig. 17 – Variation of inlet and outlet pressure inside the pipeline with an increase in the diameter of cross section of the pipeline

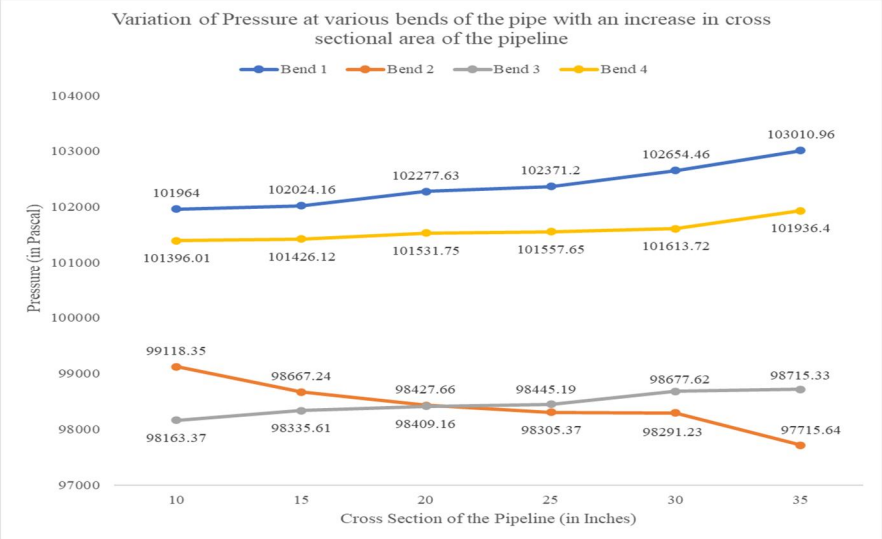

Fig. 18 – Variation pressure at various bends inside the pipeline with an increase in diameter of cross section of the pipeline

The graphs represented in fig. 16, fig. 17 and fig. 18 indicate the plot of maximum and minimum pressure inside the pipeline vs. diameter of cross section of the pipeline, pressure at the inlet and outlet of the pipe vs. diameter of cross section of the pipeline, and the pressure at various bents of the pipeline with respect to the diameter of cross section of the pipeline, respectively, which were plotted taking into consideration the values obtained from table 4. The observations made are – an increase in the size of the pipeline diameter from 10 inches to 35 inches caused the maximum velocity inside the pipeline to rise substantially from 105122 Pa to 109278 Pa, and the minimum pressure inside the pipeline to fall steeply from 96597.6 Pa to 90832.7 Pa. The pressure at the inlet of the pipeline rose notably from 105012.44 Pa to 108627.67 Pa, and the outlet pressure fell substantially from 99597.56 Pa to 94595.9 Pa. The value of pressure drop was found to be ranging between 5414.88 Pa and 14031.77 Pa, or 5.15% to 12.91%. While the pressure at bend 1 and 4 of the pipeline system were found to be increasing, while the same in bend 2 decreased and for bend 3 it increased with an increase in concentration of solid particles in slurry.

B. For Radius of Curvature of Bends – R1000

1) Variation of Pressure Drop with Varying bend Angles of the Pipeline

The variations of the angles of bends of the pipeline were done by keeping the area of cross section/outer diameter of the pipeline constant at 15 inches, and inlet velocity of slurry constant at 1.5 m/s. The inner diameter of the pipeline in all the cases was also maintained at 14.5 inches. The bend angles were varied as follows - 3°, 6°, 9°, 12°, 15°, and 18°, respectively. The radius of curvature of pipeline bend was also kept constant at R1000. The results thus obtained are shown in Table 5 below, and also plotted in graphs.

Table 5 – Variation of pressure inside the pipeline with an increase in bend angles

Bend Angles (in °)	Pressure values in the pipeline (in Pa)								
	Maximum Pressure	Minimum Pressure	Pressure at the Inlet	Pressure at the Outlet	Pressure Drop	Pressure at Bend 1	Pressure at Bend 2	Pressure at Bend 3	Pressure at Bend 4
3	105294	97298.2	103763.14	100217.01	3546.13	101468.33	100109.66	100511.26	102502.21
6	105334	95556.1	103878.05	100211.83	3666.22	101760.12	98652.7	98373	102458.56
9	105447	93829.6	105100.98	98909.63	6191.35	101974.61	97110.26	96652.11	101609.97
12	105512	92100.6	105252.38	98777.93	6474.48	102222.8	95288.9	95786.6	101476.81
15	105593	90409.5	105354.32	98766.8	6587.52	102247.62	94322.68	93876.27	101406.21
18	105688	88723.8	105443.97	98736.54	6707.43	102424.12	92886.34	92221.31	100946.06

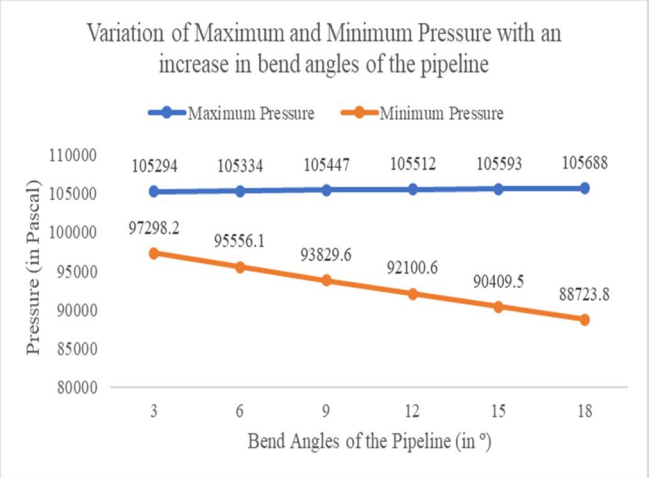

Fig. 19 – Variation of maximum and minimum pressure inside the pipe with increase in bend angles of the pipe

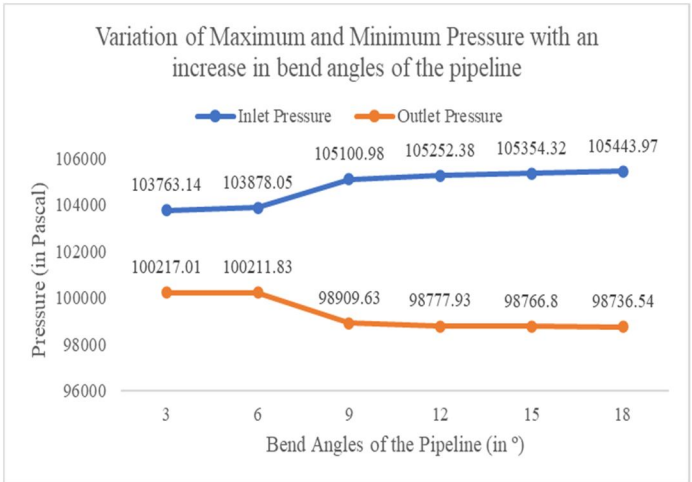

Fig. 20 – Variation of inlet and outlet pressure inside the pipeline with an increase in the bend angles of the pipe

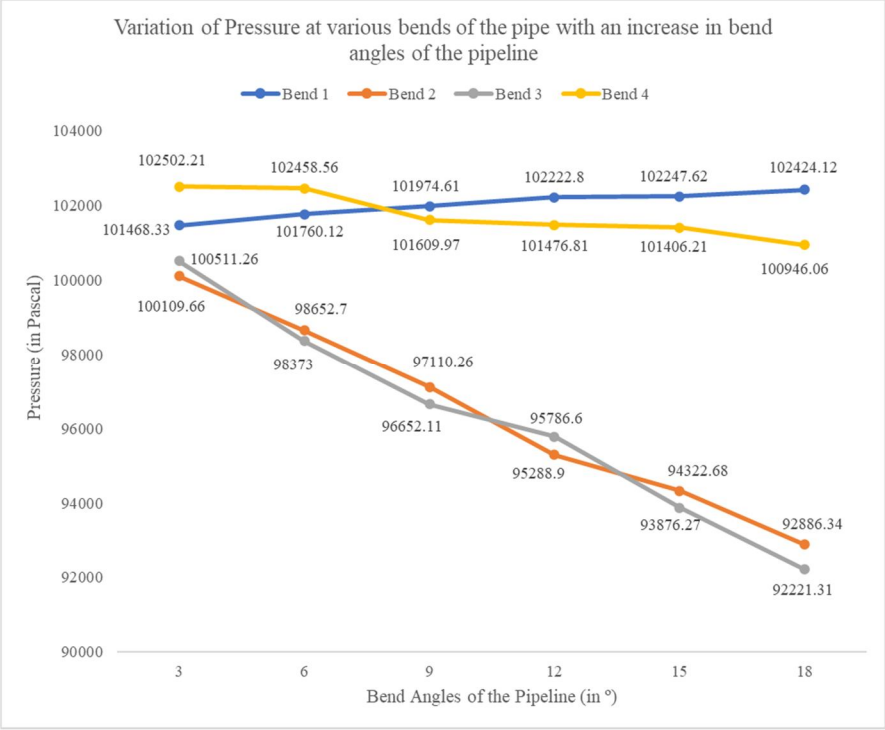

Fig. 21 – Variation pressure at various bends inside the pipeline with an increase in the bend angles of the pipe

The graphs represented in fig. 19, fig. 20 and fig. 21 indicate the plot of maximum and minimum pressure inside the pipeline vs. bend angles of the pipe system, pressure at the inlet and outlet of the pipe vs. bend angles of the pipe system, and the pressure at various bents of the pipeline with respect to the bend angles, respectively, which were plotted taking into consideration the values obtained from table 5. The observations made are – with an increase in angle of bend of the pipeline system from 3º to 18º, the maximum pressure increased marginally from 105294 Pa to 105688 Pa, and the minimum pressure dropped substantially from 97298.2 Pa to 88723.8 Pa. But the pressure at the inlet somewhat noticeably increased, from 103763.14 Pa to 105443.97 Pa and the outlet pressure decreased in a similar fashion from 100217.01 Pa to 98736.54 Pa respectively. The value of pressure drop was found to be ranging between 3546.13 Pa and 6707.43 Pa, or 3.14% to 6.36%. While the pressure at bend 1 of the pipeline system was found to be increasing, whereas, pressure at bend 4 decreased marginally and the same in bends 2 and 3 were found to be decreasing substantially with an increase in the angles of bend of the pipeline.

2) Variation of Pressure Drop with Varying Inlet Velocity of Slurry

The variations of the inlet velocity of slurry were done by keeping the area of cross section/outer diameter of the pipeline constant at 15 inches, and bend angles at 6º. The inner diameter of the pipeline in all the cases was also maintained at 14.5 inches. The inlet velocities were varied as follows – 0.5 m/s, 1.0 m/s, 1.5 m/s, 2.0 m/s, 2.5 m/s, and 3.0 m/s respectively. The radius of curvature of pipeline bend was also kept constant at R1000. The results thus obtained are shown in Table 6 below, and also plotted in graphs.

Table 6 – Variation of pressure inside the pipeline with an increase in inlet velocity of slurry

Inlet Velocity (in m/s)	Pressure values in the pipeline (in Pa)								
	Maximum Pressure	Minimum Pressure	Pressure at the Inlet	Pressure at the Outlet	Pressure Drop	Pressure at Bend 1	Pressure at Bend 2	Pressure at Bend 3	Pressure at Bend 4
0.5	104307	95239.3	104096.31	98891.62	5204.69	102033.07	98250.17	98354.44	101458.27
1.0	104723	95379	104507.27	98896.06	5611.21	102039.04	98615.05	98402.49	101513.55
1.5	105370	95604.4	105153.42	98903.85	6249.57	102353	98894.99	98480.98	101635.32
2.0	106247	95901.1	105973.37	98914.35	7054.02	103172.4	99340.24	98690.74	101778.5
2.5	107337	96258.2	107012.36	98928.86	8083.5	104242.17	100072.05	99154.83	101930.85
3.0	108657	96693.9	108267.77	98936.65	9331.12	104956.06	100890.52	99379.18	102024.43

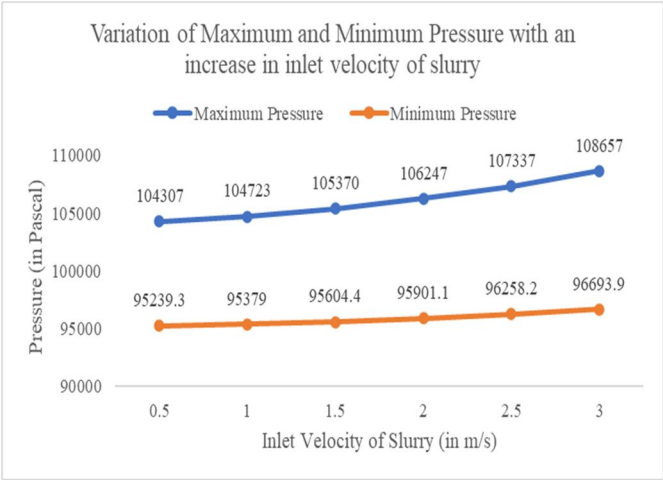

Fig. 22 – Variation of maximum and minimum pressure inside the pipe with increase in inlet velocity of slurry

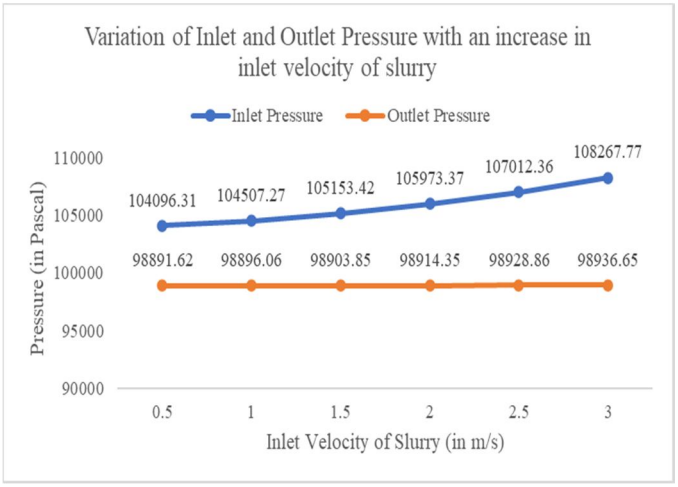

Fig. 23 – Variation of inlet and outlet pressure inside the pipeline with an increase in the inlet velocity of slurry

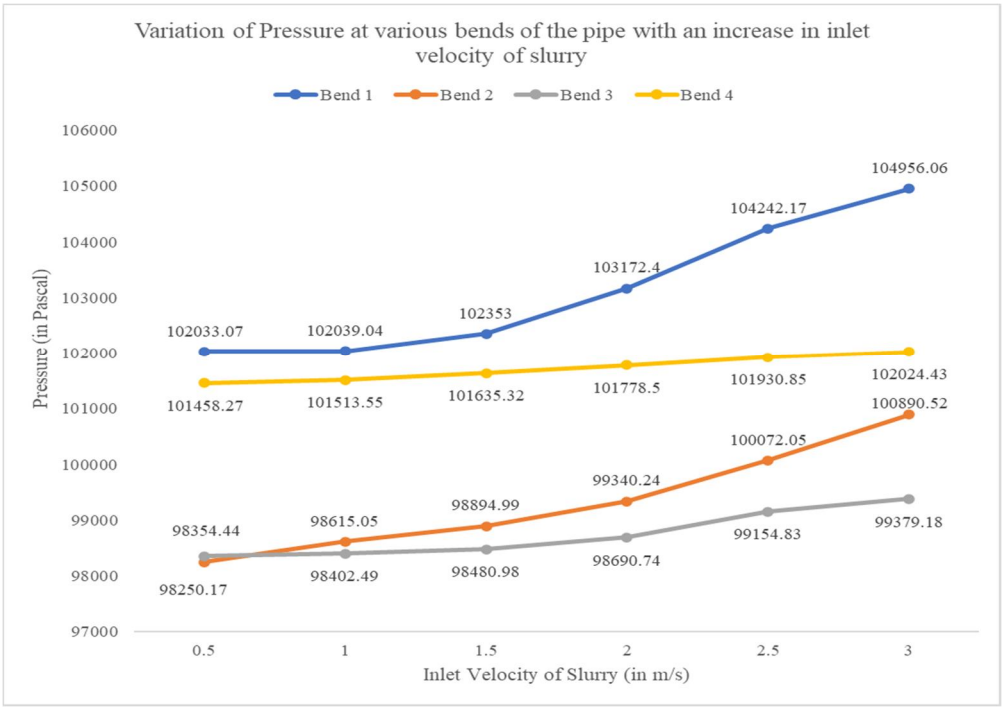

Fig. 24 – Variation pressure at various bends inside the pipeline with an increase in the inlet velocity of slurry

The graphs represented in fig. 22, fig. 23 and fig. 24 indicate the plot of maximum and minimum pressure inside the pipeline vs. inlet velocity of slurry, pressure at the inlet and outlet of the pipe vs. inlet velocity of slurry, and the pressure at various bents of the pipeline with respect to the inlet velocity of slurry, respectively, which were plotted taking into consideration the values obtained from table 6. The observations made are – with an increase in velocity at the inlet of the pipeline system from 0.5 m/s to 3 m/s, the maximum pressure increased substantially from 104307 Pa to 108657 Pa, and the minimum pressure increased minorly from 95239.3 Pa to 96693.9 Pa. Both the pressures at the inlet and the outlet increased during the process, albeit the rise in pressure at the inlet was steep, i.e., from 104096.31 Pa to 108267.77 Pa, as compared to the marginal rise in pressure at the outlet of the pipe, i.e., from 98891.6 Pa to 98936.65 Pa. The value of pressure drop was found to be ranging between 5204.69 Pa and 9331.12 Pa, or 4.99% to 8.61%. The pressure at bends at all the 4 bends were found to be increasing with an increase in the inlet velocity of slurry. While pressure at bend 1 increased rapidly, the same for bends 2 and 3 increased substantially, while for bend 4, it increased marginally.

3) Variation of Pressure Drop with Varying Concentration of solid Particles in Slurry

The variations of the concentration of solids in slurry were done by keeping the area of cross section/outer diameter of the pipeline constant at 15 inches, and inlet velocity of slurry constant at 1.5 m/s. The inner diameter of the pipeline in all the cases was also maintained at 14.5 inches. The concentration of solids in slurry were varied as follows – 30%, 40%, 50%, 60%, 70% and 80% respectively. The radius of curvature of pipeline bend was also kept constant at R1000. The results thus obtained are shown in Table 7 below, and also plotted in graphs.

Table 7 – Variation of pressure inside the pipeline with an increase in concentration of solids in slurry

Concentration of solids in slurry (in %)	Pressure values in the pipeline (in Pa)								
	Maximum Pressure	Minimum Pressure	Pressure at the Inlet	Pressure at the Outlet	Pressure Drop	Pressure at Bend 1	Pressure at Bend 2	Pressure at Bend 3	Pressure at Bend 4
30	104045	97182.6	103861.93	99593.38	4268.55	101944.67	99493.58	99422.26	101755.04
40	104289	96824.1	104110.08	99445.32	4664.76	102023.11	99423.13	99237.16	101649.17
50	104598	96445	104377.61	99298.48	5079.13	102147.14	99232.38	99012.07	101593.81
60	104989	95975	104776.79	98808.25	5968.54	102299.41	99176	98806.81	101533.12
70	105605	95444.2	105385.1	98604.76	6780.34	102741.24	99003.94	98556.09	101489.07
80	106897	94899.3	106636.14	98498.03	8138.11	103494.78	98899.65	98381.32	101449.81

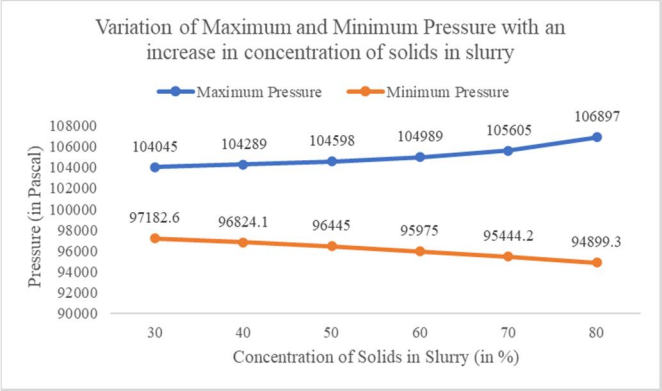

Fig. 25 – Variation of maximum and minimum pressure inside the pipe with increase in concentration of solids in slurry

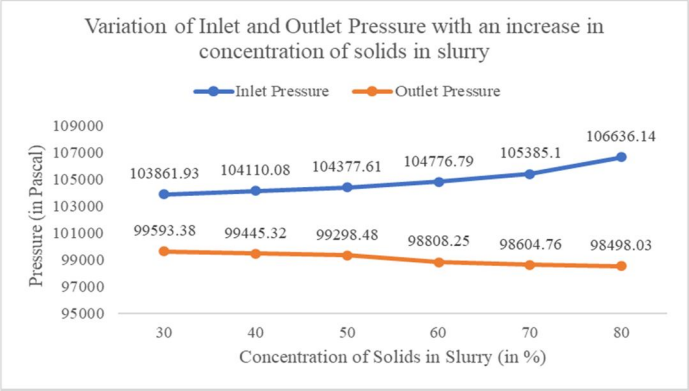

Fig. 26 – Variation of inlet and outlet pressure inside the pipeline with an increase in the concentration of solids in slurry

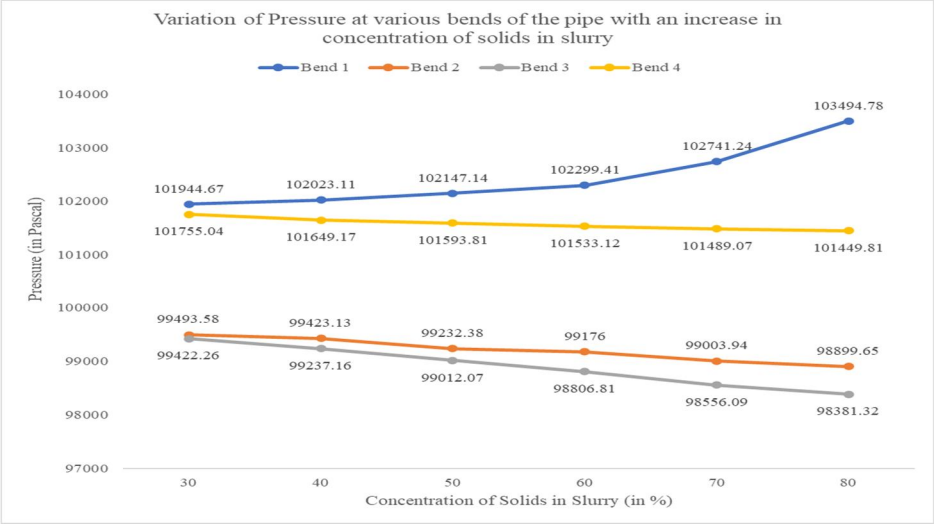

Fig. 27 – Variation pressure at various bends inside the pipeline with an increase in concentration of solids in slurry

The graphs represented in fig. 25, fig. 26 and fig. 27 indicate the plot of maximum and minimum pressure inside the pipeline vs. concentration of solids in slurry, pressure at the inlet and outlet of the pipe vs. concentration of solids in slurry, and the pressure at various bents of the pipeline with respect to the concentration of solids in slurry, respectively, which were plotted taking into consideration the values obtained from table 7. The observations made are – when the concentration of solids in the slurry flowing inside the pipeline was increased from 30% to 80%, the maximum pressure was found to be increasing from 104045 Pa to 106897 Pa, while the minimum pressure inside the pipeline decreased notably from 97182.6 Pa to 94899.3 Pa. Also, while the inlet pressure varied in the same manner as the maximum pressure, slow initially and steeper afterwards, from 103861.93 Pa to 106636.14 Pa, the outlet pressure fell minorly during the process, from 99593.38 Pa to 98498.03 Pa. The value of pressure drop was found to be ranging between 4268.55 Pa and 8138.11 Pa, or 4.1% to 7.63%. While the pressure at bend 1 of the pipeline system were found to be increasing rapidly, the same for bend 4 was found to be falling albeit slowly, while the same in bends 2 and 3 were found to be decreasing, though for bend 2, it decreased slowly and for bend 3 it decreased rapidly with an increase in concentration of solid particles in slurry.

4) Variation of Pressure drop with Varying Diameter of Cross Section of Pipeline

The variations of the diameter of cross section of the pipeline were done by keeping the bend angles of the pipe constant at 6º, and inlet velocity of slurry constant at 1.5 m/s. The inner diameter of the pipeline in all the cases was also maintained at 0.5 inches less than the outer diameter. The diameter of cross section of the pipeline were varied as follows – 10 inches, 15 inches, 20 inches, 25 inches, 30 inches, 35 inches respectively. The radius of curvature of pipeline bend was also kept constant at R1000. The results thus obtained are shown in Table 8 below, and also plotted in graphs.

Table 8 – Variation of pressure inside the pipe with an increase in diameter of cross section of pipe

Diameter of the pipeline (in Inches)	Pressure values in the pipeline (in Pa)								
	Maximum Pressure	Minimum Pressure	Pressure at the Inlet	Pressure at the Outlet	Pressure Drop	Pressure at Bend 1	Pressure at Bend 2	Pressure at Bend 3	Pressure at Bend 4
10	105106	96597.2	104933.79	99624.16	5309.63	102917.52	99118.72	98562.03	101845.93
15	105486	95350.8	105246.04	98653.83	6592.21	102513.89	98819.11	98461.18	101791.17
20	106296	94177.5	105923.13	97654.08	8269.05	102462.49	98766.54	98393.88	101575.26
25	107232	93031.6	106751.19	96642.9	10108.29	102223.75	98751.66	98347.2	101495.17
30	108224	91919.8	107663.42	95577.87	12085.55	101994.77	98726.53	97823.42	101357.5
35	109245	90828.6	108619.79	94620.97	13998.82	101694.12	98655.82	97755.77	101266.28

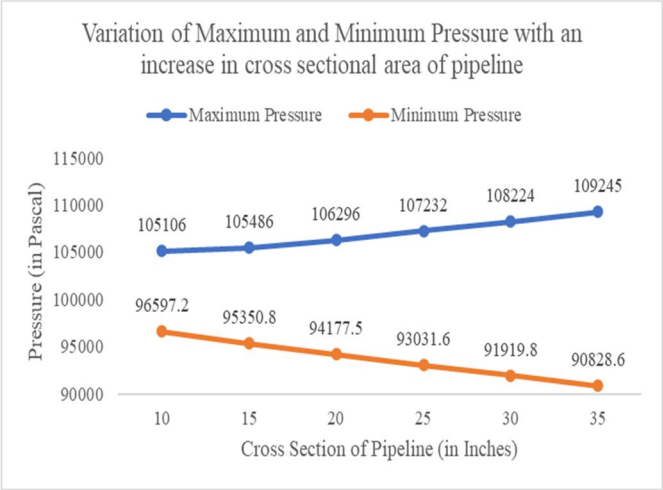

Fig. 28 – Variation of maximum and minimum pressure inside the pipe with increase in diameter of cross section of the pipeline

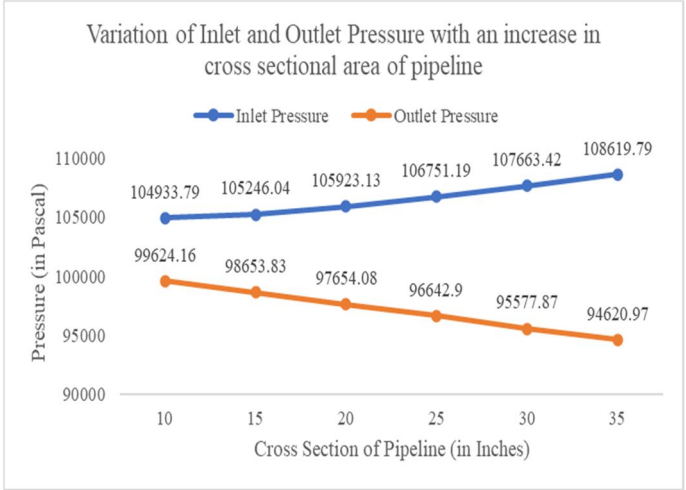

Fig. 29 – Variation of inlet and outlet pressure inside the pipeline with an increase in the diameter of cross section of the pipeline

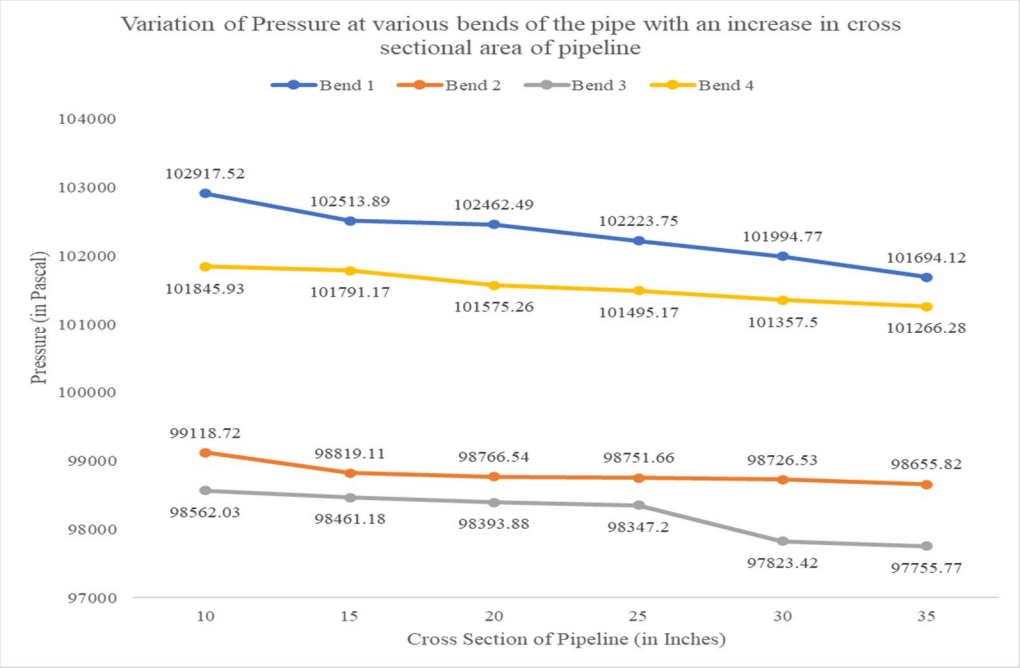

Fig. 30 – Variation pressure at various bends inside the pipe with an increase in diameter of cross section of pipeline

The graphs represented in fig. 28, fig. 29 and fig. 30 indicate the plot of maximum and minimum pressure inside the pipeline vs. diameter of cross section of the pipeline, pressure at the inlet and outlet of the pipe vs. diameter of cross section of the pipeline, and the pressure at various bents of the pipeline with respect to the diameter of cross section of the pipeline, respectively, which were plotted taking into consideration the values obtained from table 8. The observations made are – an increase in the size of the pipeline diameter from 10 inches to 35 inches caused the maximum velocity inside the pipeline to rise substantially from 105106 Pa to 109245 Pa, and the minimum pressure inside the pipeline to fall steeply from 96597.2 Pa to 90828.6 Pa. The pressure at the inlet of the pipeline rose notably from 104933.79 Pa to 108619.79 Pa, and the outlet pressure fell substantially from 99624.16 Pa to 94620.97 Pa. The value of pressure drop was found to be ranging between 5309.63 Pa and 13998.82 Pa, or 5.05% to 12.88%. While the pressure at all the four bends were found to be decreasing, the pressure values at bends 2 and 4 decreased slowly, the same for bend 1 decreased steeply, and the same for bend 3 fell marginally till a cross section of 25 inches, after which, it fell drastically with an increase in concentration of solid particles in slurry.

C. For Radius of Curvature of Bends – R1500

1) Variation of Pressure drop with Varying bend Angles of the Pipeline

The variations of the angles of bends of the pipeline were done by keeping the area of cross section/outer diameter of the pipeline constant at 15 inches, and inlet velocity of slurry constant at 1.5 m/s. The inner diameter of the pipeline in all the cases was also maintained at 14.5 inches. The bend angles were varied as follows - 3°, 6°, 9°, 12°, 15°, and 18°, respectively. The radius of curvature of pipeline bend was also kept constant at R1500. The results thus obtained are shown in Table 9 below, and also plotted in graphs.

Table 9 – Variation of pressure inside the pipeline with an increase in bend angles

Bend Angles (in °)	Pressure values in the pipeline (in Pa)								
	Maximum Pressure	Minimum Pressure	Pressure at the Inlet	Pressure at the Outlet	Pressure Drop	Pressure at Bend 1	Pressure at Bend 2	Pressure at Bend 3	Pressure at Bend 4
3	105297	97300.8	103792.13	100170.18	3621.95	101292.08	100026.36	100517.95	101004.96
6	105333	95555.2	103871	100107.22	3763.78	101716.47	99053.02	98229.71	101210.31
9	105369	93802.8	105119.38	98891.64	6227.74	101937.11	97240.42	97062.13	101468.55
12	105408	92076	105216.81	98772.55	6444.26	102105.49	95272.52	95826.45	102210.31
15	105428	90349.7	105266.3	98766.18	6500.12	102191.07	94220.48	93831.59	102226.35
18	105436	88676.9	105279.29	98735.13	6544.16	102502.52	92522.68	92298.75	102335.71

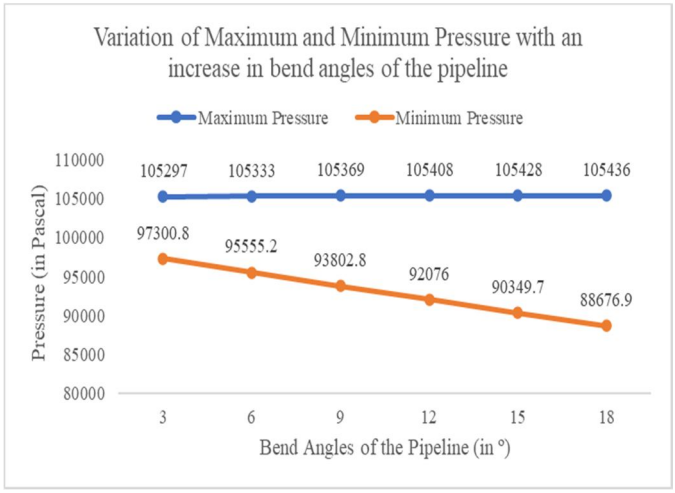

Fig. 31 – Variation of maximum and minimum pressure inside the pipe with increase in bend angles of the pipe

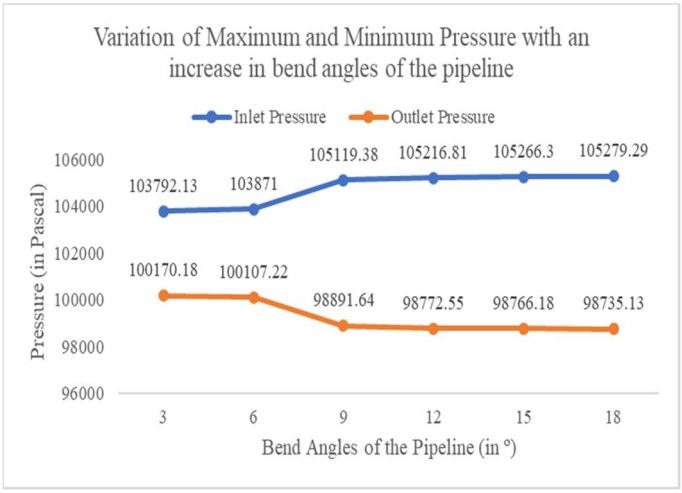

Fig. 32 – Variation of inlet and outlet pressure inside the pipeline with an increase in the bend angles of the pipe

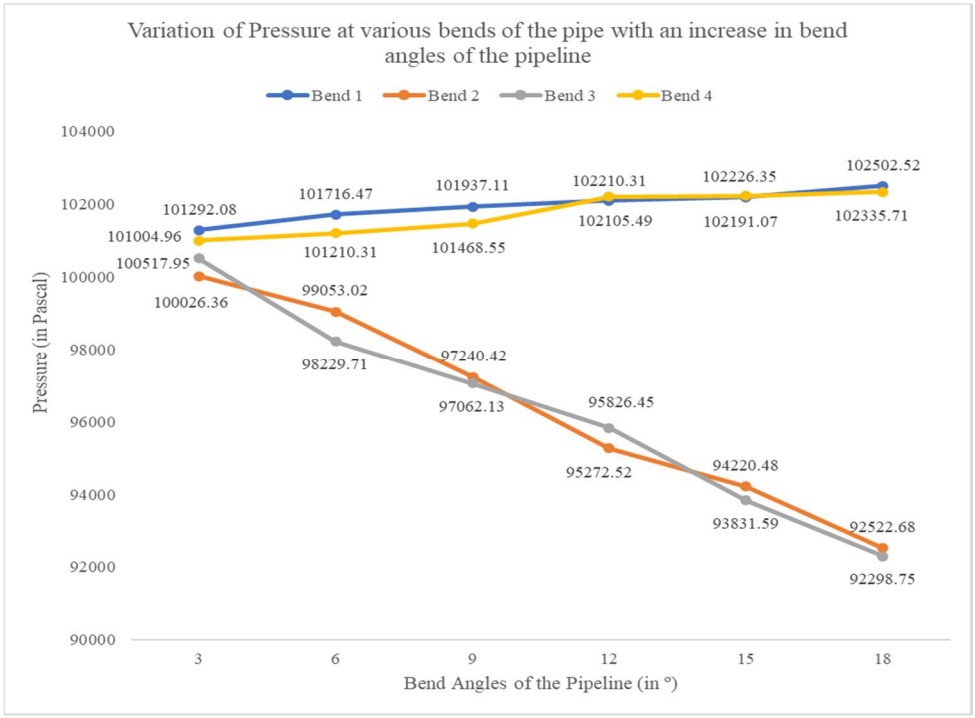

Fig. 33 – Variation pressure at various bends inside the pipeline with an increase in the bend angles of the pipe

The graphs represented in fig. 31, fig. 32 and fig. 33 indicate the plot of maximum and minimum pressure inside the pipeline vs. bend angles of the pipe system, pressure at the inlet and outlet of the pipe vs. bend angles of the pipe system, and the pressure at various bents of the pipeline with respect to the bend angles, respectively, which were plotted taking into consideration the values obtained from table 9. The observations made are – with an increase in angle of bend of the pipeline system from 3º to 18º, the maximum pressure increased marginally from 105297 Pa to 105436 Pa, and the minimum pressure dropped substantially from 97300.8 Pa to 88676.9 Pa. But the pressure at the inlet somewhat noticeably increased, from 103792.13 Pa to 105279.29 Pa and the outlet pressure decreased in a similar fashion from 100170.18 Pa to 98735.13 Pa respectively. The value of pressure drop was found to be ranging between 3621.95 Pa and 6544.16 Pa, or 3.48% to 6.21%. While the pressure at bends 1 and 4 of the pipeline system was found to be increasing, the same in bends 2 and 3 were found to be decreasing substantially with an increase in the angles of bend of the pipeline.

2) Variation of Pressure Drop with Varying inlet Velocity of Slurry

The variations of the inlet velocity of slurry were done by keeping the area of cross section/outer diameter of the pipeline constant at 15 inches, and bend angles at 6º. The inner diameter of the pipeline in all the cases was also maintained at 14.5 inches. The inlet velocities were varied as follows – 0.5 m/s, 1.0 m/s, 1.5 m/s, 2.0 m/s, 2.5 m/s, and 3.0 m/s respectively. The radius of curvature of pipeline bend was also kept constant at R1500. The results thus obtained are shown in Table 10 below, and also plotted in graphs.

Table 10 – Variation of pressure inside the pipeline with an increase in inlet velocity of slurry

Inlet Velocity (in m/s)	Pressure values in the pipeline (in Pa)								
	Maximum Pressure	Minimum Pressure	Pressure at the Inlet	Pressure at the Outlet	Pressure Drop	Pressure at Bend 1	Pressure at Bend 2	Pressure at Bend 3	Pressure at Bend 4
0.5	104303	95235.9	104093.42	98890.35	5203.07	101432.18	98121.55	98294.39	101300.03
1.0	104716	95374.6	104505.43	98892.12	5613.31	101735.71	98504.45	98341.01	101592.03
1.5	105365	95599.5	105150.79	98893.05	6257.74	102493.61	99069.39	98587.69	101628.4
2.0	106196	95890	105979	98899.05	7079.95	103040.87	99424.56	98723.56	101656.05
2.5	107245	96252.01	107016.46	98910.08	8106.38	104004.1	100083.05	99217.31	102131.91
3.0	108806	96692.1	108258.96	98934.79	9324.17	105192.89	100978.33	99489.99	102239.32

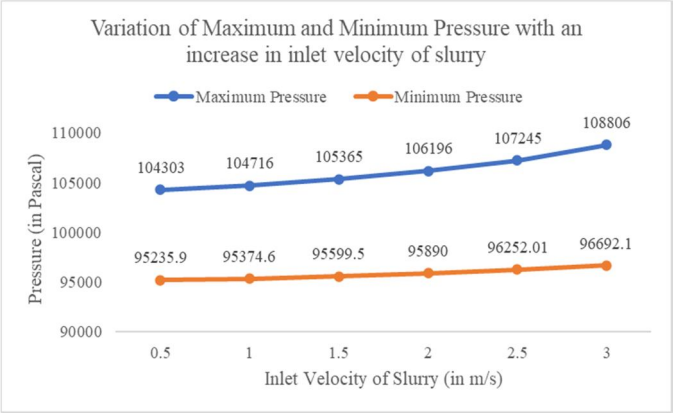

Fig. 34 – Variation of maximum and minimum pressure inside the pipe with increase in inlet velocity of slurry

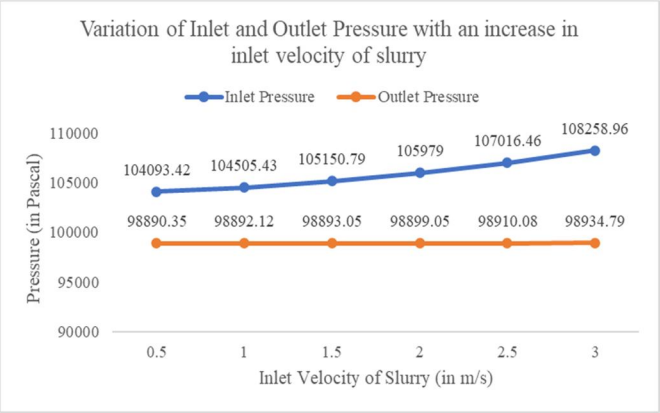

Fig. 35 – Variation of inlet and outlet pressure inside the pipeline with an increase in the inlet velocity of slurry

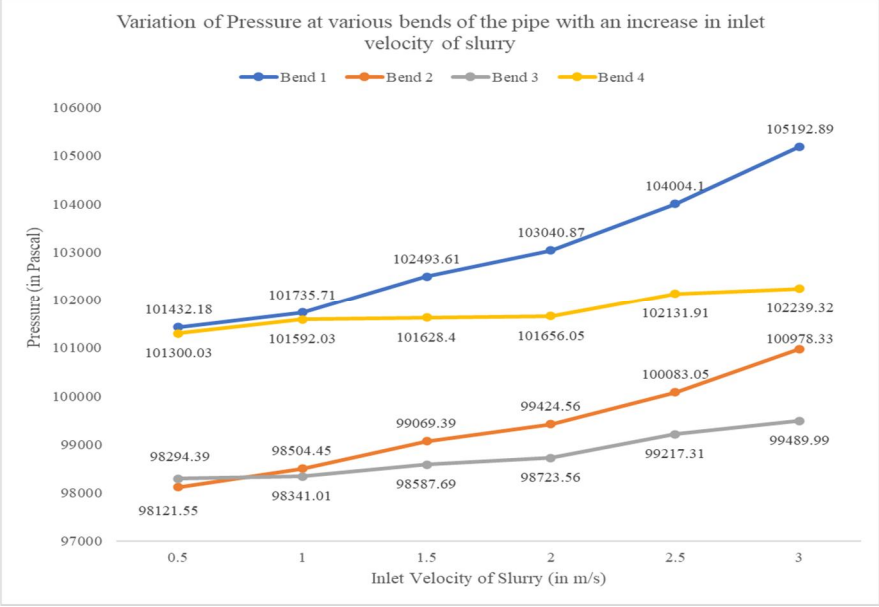

Fig. 36 – Variation pressure at various bends inside the pipeline with an increase in the inlet velocity of slurry

The graphs represented in fig. 34, fig. 35 and fig. 36 indicate the plot of maximum and minimum pressure inside the pipeline vs. inlet velocity of slurry, pressure at the inlet and outlet of the pipe vs. inlet velocity of slurry, and the pressure at various bents of the pipeline with respect to the inlet velocity of slurry, respectively, which were plotted taking into consideration the values obtained from table 10. The observations made are – with an increase in velocity at the inlet of the pipeline system from 0.5 m/s to 3 m/s, the maximum pressure increased substantially from 104303 Pa to 108806 Pa, and the minimum pressure increased minorly from 95235.9 Pa to 96692.1 Pa. Both the pressures at the inlet and the outlet increased during the process, albeit the rise in pressure at the inlet was steep, i.e., from 104093.42 Pa to 108258.96 Pa, as compared to the marginal rise in pressure at the outlet of the pipe, i.e., from 98890.35 Pa to 98934.79 Pa. The value of pressure drop was found to be ranging between 5203.07 Pa and 9324.17 Pa, or 4.99% to 8.61%. The pressure at bends at all the 4 bends were found to be increasing with an increase in the inlet velocity of slurry. While pressure at bend 1 increased rapidly, the same for bends 2 and 3 increased substantially, while for bend 4, it increased marginally.

3) Variation of Pressure drop with Varying Concentration of Solid Particles in Slurry

The variations of the concentration of solids in slurry were done by keeping the area of cross section/outer diameter of the pipeline constant at 15 inches, and inlet velocity of slurry constant at 1.5 m/s. The inner diameter of the pipeline in all the cases was also maintained at 14.5 inches. The concentration of solids in slurry were varied as follows – 30%, 40%, 50%, 60%, 70% and 80% respectively. The radius of curvature of pipeline bend was also kept constant at R1500. The results thus obtained are shown in Table 11 below, and also plotted in graphs.

Table 11 – Variation of pressure inside the pipe with an increase in concentration of solids in slurry

Concentration of solids in slurry (in %)	Pressure values in the pipeline (in Pa)								
	Maximum Pressure	Minimum Pressure	Pressure at the Inlet	Pressure at the Outlet	Pressure Drop	Pressure at Bend 1	Pressure at Bend 2	Pressure at Bend 3	Pressure at Bend 4
30	104014	97180.6	103861.39	99589.91	4271.48	102001.11	99547.37	99333.86	101520.47
40	104275	96824.6	104108.93	99445.05	4663.88	102050.24	99402.32	99291.79	101550.67
50	104575	96445.6	104394.13	99274.28	5119.85	102119.8	99394.84	99274.95	101652.73
60	104975	95973	104777.85	99067.53	5710.32	102521.13	99331.38	99201.48	101692.12
70	105600	94895.6	105378.81	98809.79	6569.02	102963.81	99295.16	98512.72	101721.15
80	106890	94439.2	106633.29	98491.47	8141.82	103581.57	98991.67	98431.72	101977.76

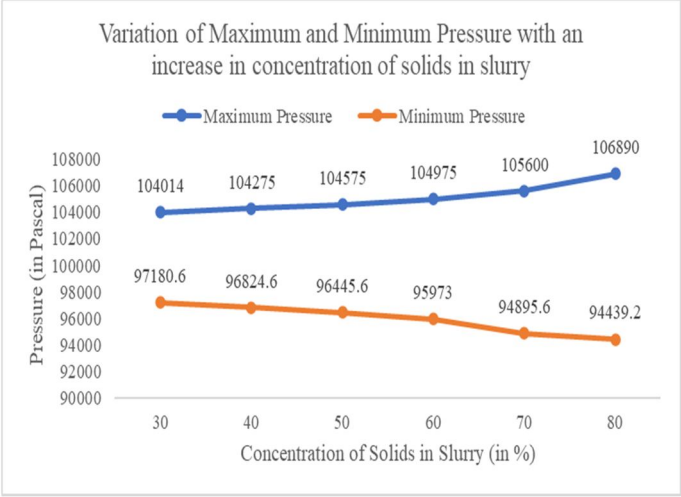

Fig. 37 – Variation of maximum and minimum pressure inside the pipe with increase in concentration of solids in slurry

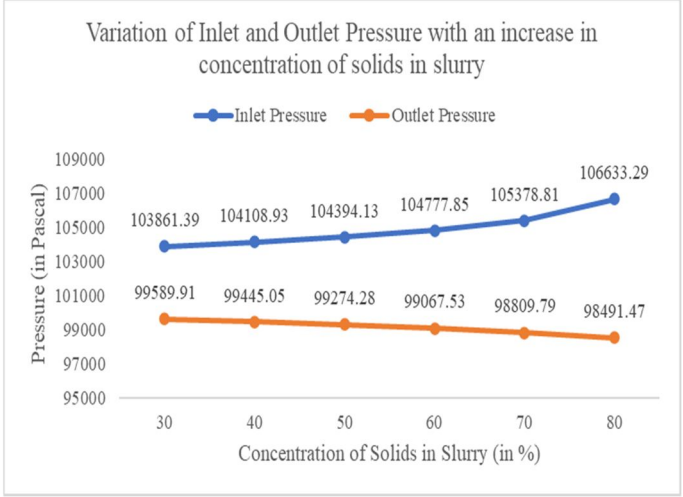

Fig. 38 – Variation of inlet and outlet pressure inside the pipeline with an increase in the concentration of solids in slurry

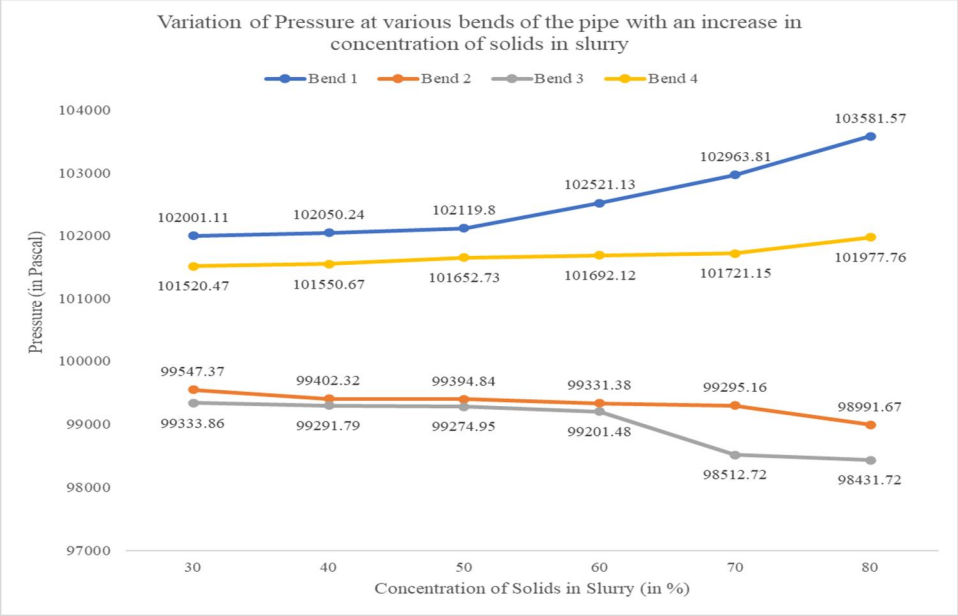

Fig. 39 – Variation pressure at various bends inside the pipeline with an increase in concentration of solids in slurry

The graphs represented in fig. 37, fig. 38 and fig. 39 indicate the plot of maximum and minimum pressure inside the pipeline vs. concentration of solids in slurry, pressure at the inlet and outlet of the pipe vs. concentration of solids in slurry, and the pressure at various bents of the pipeline with respect to the concentration of solids in slurry, respectively, which were plotted taking into consideration the values obtained from table 11. The observations made are – when the concentration of solids in the slurry flowing inside the pipeline was increased from 30% to 80%, the maximum pressure was found to be increasing from 104014 Pa to 106890 Pa, while the minimum pressure inside the pipeline decreased notably from 97180.6 Pa to 94439.2 Pa. Also, while the inlet pressure varied in the same manner as the maximum pressure, slow initially and steeper afterwards, from 103861.93 Pa to 106633.29 Pa, the outlet pressure fell minorly during the process, from 99589.91 Pa to 98491.4 Pa. The value of pressure drop was found to be ranging between 4271.48 Pa and 8141.82 Pa, or 4.11% to 7.63%. While the pressure at bend 1 of the pipeline system were found to be increasing rapidly, the same for bend 4 was found to be falling albeit slowly, while the same in bends 2 and 3 were found to be decreasing, though for bend 2, it decreased slowly and for bend 3 it decreased rapidly after 60% solids concentration, with an increase in concentration of solid particles in slurry.

4) Variation of Pressure Drop with Varying Diameter of Cross Section of Pipeline

The variations of the diameter of cross section of the pipeline were done by keeping the bend angles of the pipe constant at 6º, and inlet velocity of slurry constant at 1.5 m/s. The inner diameter of the pipeline in all the cases was also maintained at 0.5 inches less than the outer diameter. The diameter of cross section of the pipeline were varied as follows – 10 inches, 15 inches, 20 inches, 25 inches, 30 inches, 35 inches respectively. The radius of curvature of pipeline bend was also kept constant at R1500. The results thus obtained are shown in Table 12 below, and also plotted in graphs.

Table 12 – Variation of pressure inside the pipe with an increase in diameter of cross section of pipe

Diameter of the pipeline (in Inches)	Pressure values in the pipeline (in Pa)								
	Maximum Pressure	Minimum Pressure	Pressure at the Inlet	Pressure at the Outlet	Pressure Drop	Pressure at Bend 1	Pressure at Bend 2	Pressure at Bend 3	Pressure at Bend 4
10	105100	96597.9	104993.6	99596.47	5397.13	102792.19	99439.03	98749.23	101992.21
15	105462	95364	105253.74	98646.46	6607.28	102720.96	98728.79	98661.74	101742.17
20	106253	94173.3	105922.7	97656	8266.7	102031.72	98533.92	98623.21	101669.07
25	107209	93029	106752.44	96628.68	10123.76	101925.89	98513.83	98610.48	101518.16
30	108192	91918.7	107673.04	95564.63	12108.41	101782.01	98291.52	98407.15	101402.18
35	109224	90829.4	108632.18	94589.33	14042.85	101342.67	98186.67	97987.53	101370.64

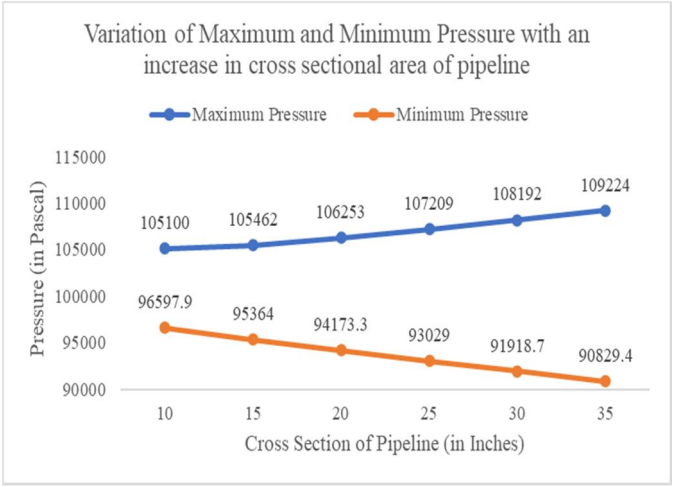

Fig. 40 – Variation of maximum and minimum pressure inside the pipe with increase in diameter of cross section of the pipeline

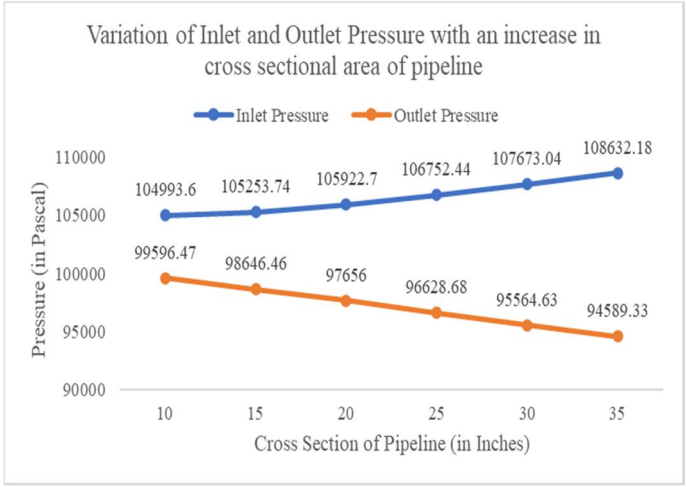

Fig. 41 – Variation of inlet and outlet pressure inside the pipeline with an increase in the diameter of cross section of the pipeline

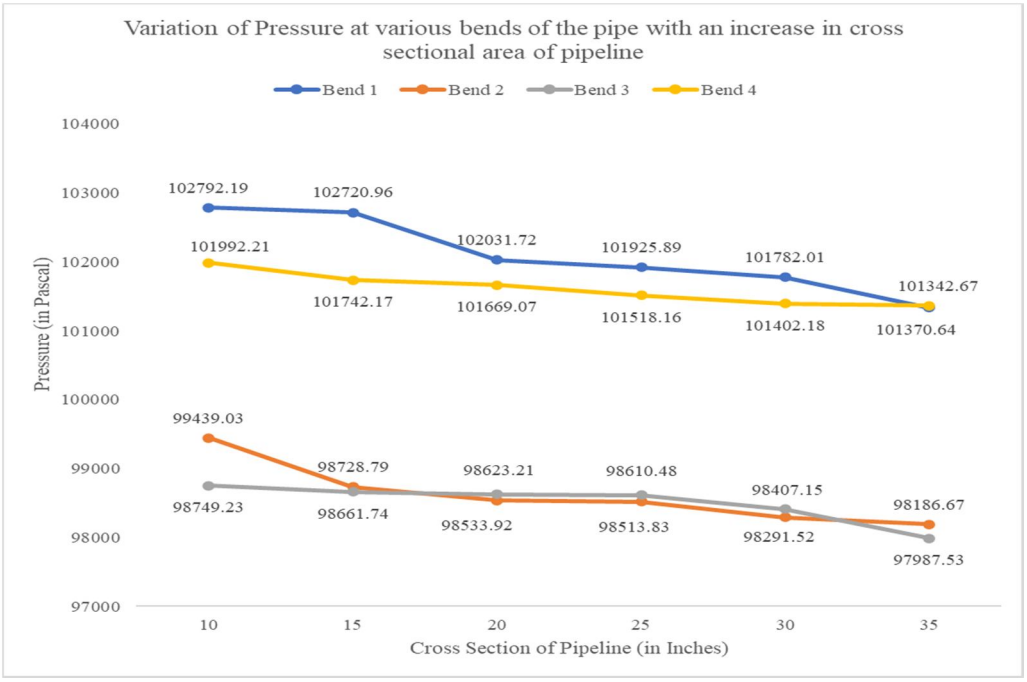

Fig. 42 – Variation pressure at various bends inside the pipe with an increase in diameter of cross section of pipeline

The graphs represented in fig. 40, fig. 41 and fig. 42 indicate the plot of maximum and minimum pressure inside the pipeline vs. diameter of cross section of the pipeline, pressure at the inlet and outlet of the pipe vs. diameter of cross section of the pipeline, and the pressure at various bents of the pipeline with respect to the diameter of cross section of the pipeline, respectively, which were plotted taking into consideration the values obtained from table 12. The observations made are – an increase in the size of the pipeline diameter from 10 inches to 35 inches caused the maximum velocity inside the pipeline to rise substantially from 105100 Pa to 109224 Pa, and the minimum pressure inside the pipeline to fall steeply from 96597.9 Pa to 90829.4 Pa. The pressure at the inlet of the pipeline rose notably from 104933.6 Pa to 108632.18 Pa, and the outlet pressure fell substantially from 99596.47 Pa to 94589.33 Pa. The value of pressure drop was found to be ranging between 5397.13 Pa and 14042.85 Pa, or 5.14% to 12.92%. While the pressure at all the four bends were found to be decreasing, the pressure values at bends 2, 3 and 4 decreased slowly, the same for bend 1 decreased steeply with an increase in concentration of solid particles in slurry.

D. For Radius of Curvature of Bends – R2000

1) Variation of Pressure Drop with Varying bend Angles of the Pipeline

The variations of the angles of bends of the pipeline were done by keeping the area of cross section/outer diameter of the pipeline constant at 15 inches, and inlet velocity of slurry constant at 1.5 m/s. The inner diameter of the pipeline in all the cases was also maintained at 14.5 inches. The bend angles were varied as follows - 3°, 6°, 9°, 12°, 15°, and 18°, respectively. The radius of curvature of pipeline bend was also kept constant at R2000. The results thus obtained are shown in Table 13 below, and also plotted in graphs.

Table 13 – Variation of pressure inside the pipeline with an increase in bend angles

Bend Angles (in º)	Pressure values in the pipeline (in Pa)								
	Maximum Pressure	Minimum Pressure	Pressure at the Inlet	Pressure at the Outlet	Pressure Drop	Pressure at Bend 1	Pressure at Bend 2	Pressure at Bend 3	Pressure at Bend 4
3	105293	97300.4	103788.46	100176.02	3612.44	101167.65	100027	100581.52	102543.07
6	105325	95550.7	103856.23	100142.17	3714.06	101524.73	99064.36	98694.48	102006.15
9	105352	93799.7	105106.8	98940.25	6166.55	102393.11	97393.22	96950.52	101714.19
12	105371	92052	105198.14	98879.51	6318.63	102553.82	95753.73	96271.97	101357.81
15	105394	90338.1	105238	98780.81	6457.19	102763.96	94011.16	94324.84	101172.5
18	105404	88673.4	105321.96	98729.15	6592.81	102863.14	92768.58	92279.52	100899.67

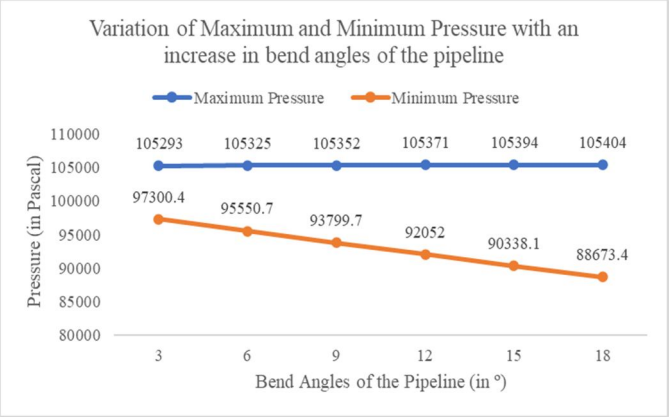

Fig. 43 – Variation of maximum and minimum pressure inside the pipe with increase in bend angles of the pipe

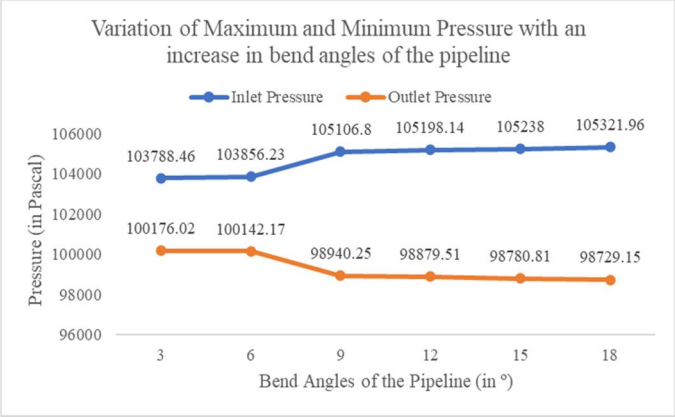

Fig. 44 – Variation of inlet and outlet pressure inside the pipeline with an increase in the bend angles of the pipe

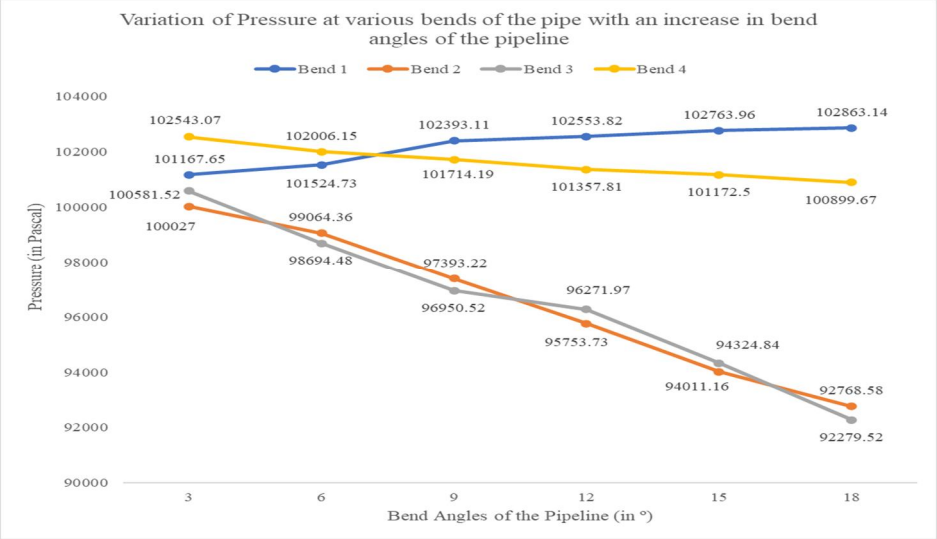

Fig. 45 – Variation pressure at various bends inside the pipeline with an increase in the bend angles of the pipe

The graphs represented in fig. 43, fig. 44 and fig. 45 indicate the plot of maximum and minimum pressure inside the pipeline vs. bend angles of the pipe system, pressure at the inlet and outlet of the pipe vs. bend angles of the pipe system, and the pressure at various bents of the pipeline with respect to the bend angles, respectively, which were plotted taking into consideration the values obtained from table 13. The observations made are – with an increase in angle of bend of the pipeline system from 3º to 18º, the maximum pressure increased marginally from 105293 Pa to 105404 Pa, and the minimum pressure dropped substantially from 97300.4 Pa to 88673.4 Pa. But the pressure at the inlet somewhat noticeably increased, from 103788.46 Pa to 105321.96 Pa and the outlet pressure decreased in a similar fashion from 100176.02 Pa to 98729.15 Pa respectively. The value of pressure drop was found to be ranging between 3612.44 Pa and 6592.81 Pa, or 3.48% to 6.25%. While the pressure at bend 1 of the pipeline system was found to be increasing, pressure at bend 4 dropped minorly, while the same in bends 2 and 3 were found to be decreasing substantially with an increase in the angles of bend of the pipeline.

2) Variation of Pressure Drop with Varying inlet Velocity of Slurry

The variations of the inlet velocity of slurry were done by keeping the area of cross section/outer diameter of the pipeline constant at 15 inches, and bend angles at 6º. The inner diameter of the pipeline in all the cases was also maintained at 14.5 inches. The inlet velocities were varied as follows – 0.5 m/s, 1.0 m/s, 1.5 m/s, 2.0 m/s, 2.5 m/s, and 3.0 m/s respectively. The radius of curvature of pipeline bend was also kept constant at R2000. The results thus obtained are shown in Table 14 below, and also plotted in graphs.

Table 14 – Variation of pressure inside the pipeline with an increase in inlet velocity of slurry

Inlet Velocity (in m/s)	Pressure values in the pipeline (in Pa)								
	Maximum Pressure	Minimum Pressure	Pressure at the Inlet	Pressure at the Outlet	Pressure Drop	Pressure at Bend 1	Pressure at Bend 2	Pressure at Bend 3	Pressure at Bend 4
0.5	104302	95231.5	104093.45	98918.97	5174.48	101431.32	98432.76	98142.32	101418.66
1.0	104710	95373.7	104499.81	98910.25	5589.56	101968.34	98572.64	98426.22	101648.69
1.5	105349	95588.7	105131.29	98908.59	6222.7	102386.35	98955.95	98686.89	101683.61
2.0	106183	95883	105950.77	98903.84	7046.93	102991.06	99358.97	98798.82	101784.68
2.5	107237	96251.6	107012.26	98896.42	8115.84	103874.57	100111.38	99189.76	101986.74
3.0	108489	96691.5	108257.15	98882.35	9374.8	105006.18	100836.84	100165.78	102246.44

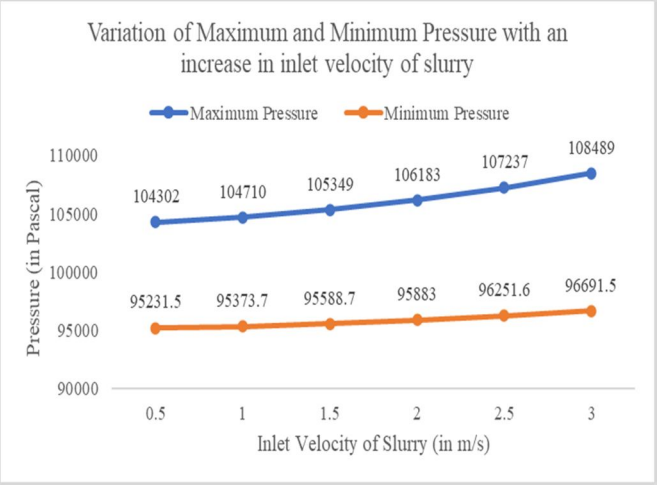

Fig. 46 – Variation of maximum and minimum pressure inside the pipe with increase in inlet velocity of slurry

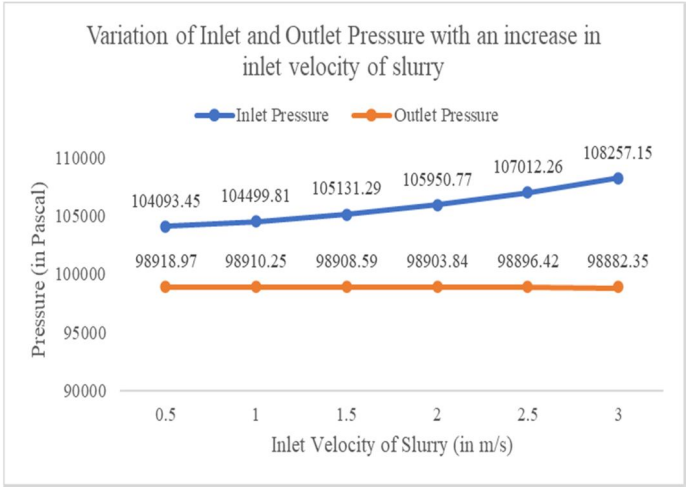

Fig. 47 – Variation of inlet and outlet pressure inside the pipeline with an increase in the inlet velocity of slurry

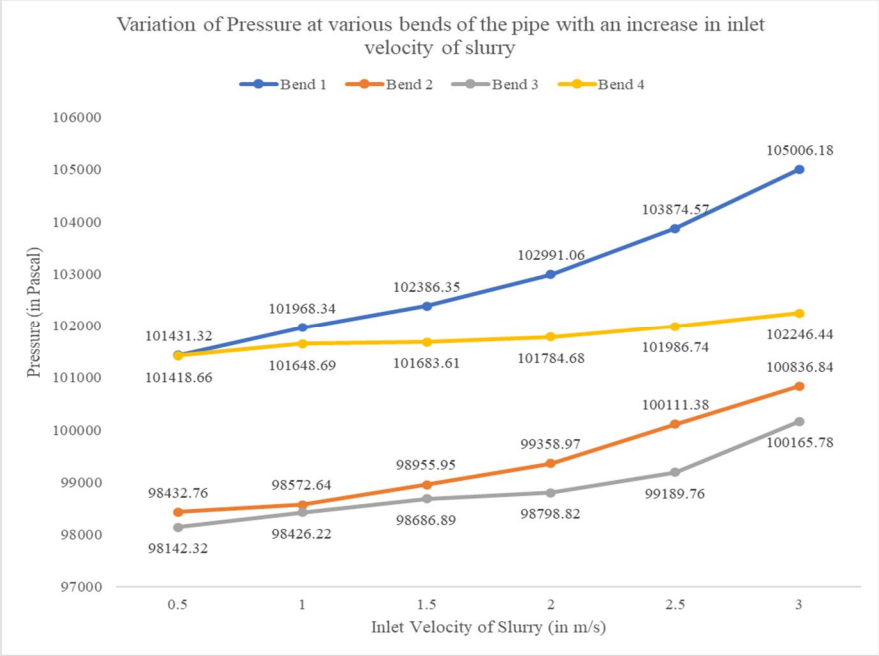

Fig. 48 – Variation pressure at various bends inside the pipeline with an increase in the inlet velocity of slurry

The graphs represented in fig. 46, fig. 47 and fig. 48 indicate the plot of maximum and minimum pressure inside the pipeline vs. inlet velocity of slurry, pressure at the inlet and outlet of the pipe vs. inlet velocity of slurry, and the pressure at various bents of the pipeline with respect to the inlet velocity of slurry, respectively, which were plotted taking into consideration the values obtained from table 14. The observations made are – with an increase in velocity at the inlet of the pipeline system from 0.5 m/s to 3 m/s, the maximum pressure increased substantially from 104302 Pa to 108489 Pa, and the minimum pressure increased minorly from 95231.5 Pa to 96691.5 Pa. The pressure at the inlet increased during the process, albeit the rise in pressure at the inlet was steep, i.e., from 104093.45 Pa to 108257.15 Pa, as compared to the marginal fall in pressure at the outlet of the pipe, i.e., from 98918.97 Pa to 98882.35 Pa. The value of pressure drop was found to be ranging between 5174.48 Pa and 9374.8 Pa, or 4.97% to 8.65%. The pressure at bends at all the 4 bends were found to be increasing with an increase in the inlet velocity of slurry. While pressure at bend 1 increased rapidly, the same for bends 2 and 3 increased substantially, while for bend 4, it increased marginally.

3) Variation of Pressure Drop with Varying Concentration of Solid Particles in Slurry

The variations of the concentration of solids in slurry were done by keeping the area of cross section/outer diameter of the pipeline constant at 15 inches, and inlet velocity of slurry constant at 1.5 m/s. The inner diameter of the pipeline in all the cases was also maintained at 14.5 inches. The concentration of solids in slurry were varied as follows – 30%, 40%, 50%, 60%, 70% and 80% respectively. The radius of curvature of pipeline bend was also kept constant at R2000. The results thus obtained are shown in Table 15 below, and also plotted in graphs.

Table 15 – Variation of pressure inside the pipe with an increase in concentration of solids in slurry

Concentration of solids in slurry (in %)	Pressure values in the pipeline (in Pa)								
	Maximum Pressure	Minimum Pressure	Pressure at the Inlet	Pressure at the Outlet	Pressure Drop	Pressure at Bend 1	Pressure at Bend 2	Pressure at Bend 3	Pressure at Bend 4
30	104006	97176.8	103854.57	99592.93	4261.64	101833.85	99483.87	99369.54	101400.69
40	104266	96818.8	104102.93	99444.37	4658.56	101846.55	99480.26	99288.06	101491.4
50	104567	96439.1	104388.22	99271.74	5116.48	102274.54	99471.33	99164.84	101516.33
60	104959	95964.2	104759.06	99063.94	5695.12	102432.45	99462.02	99058.29	101580.78
70	105578	95426.5	105358.63	98809.81	6548.82	102507.2	99402.15	98937.67	101625.1
80	106879	94894	106616.97	98493.91	8123.06	103325.71	99351.06	98494.2	102115.67

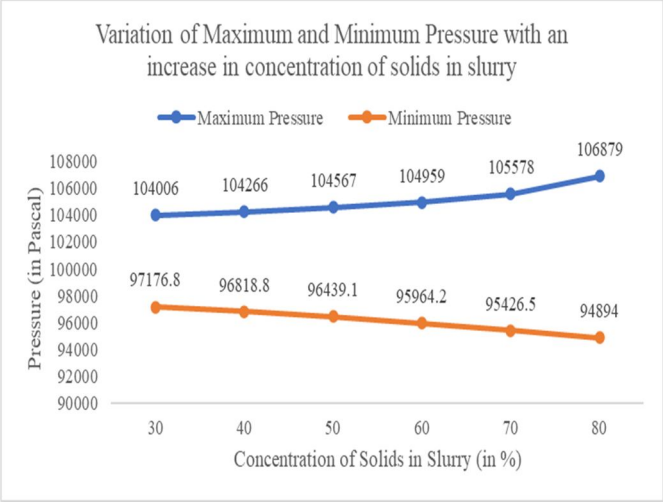

Fig. 49 – Variation of maximum and minimum pressure inside the pipe with increase in concentration of solids in slurry

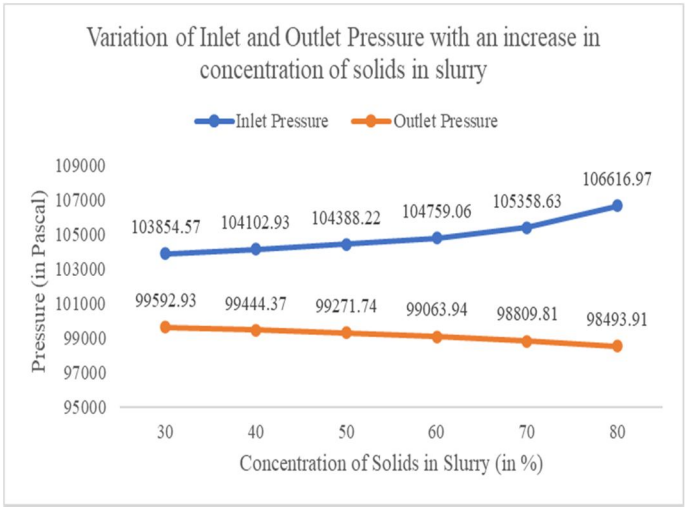

Fig. 50 – Variation of inlet and outlet pressure inside the pipeline with an increase in the concentration of solids in slurry

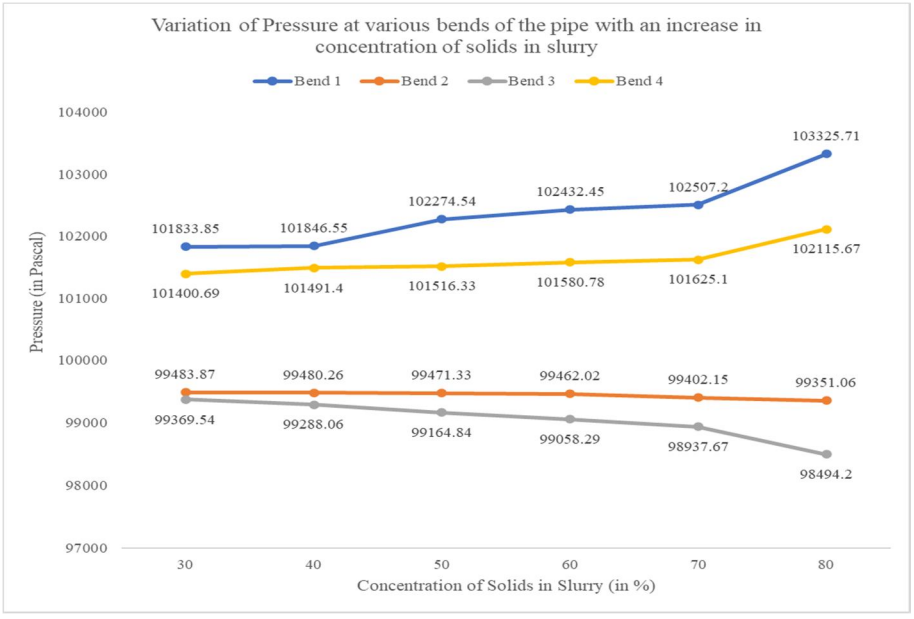

Fig. 51 – Variation pressure at various bends inside the pipeline with an increase in concentration of solids in slurry

The graphs represented in fig. 49, fig. 50 and fig. 51 indicate the plot of maximum and minimum pressure inside the pipeline vs. concentration of solids in slurry, pressure at the inlet and outlet of the pipe vs. concentration of solids in slurry, and the pressure at various bents of the pipeline with respect to the concentration of solids in slurry, respectively, which were plotted taking into consideration the values obtained from table 15. The observations made are – when the concentration of solids in the slurry flowing inside the pipeline was increased from 30% to 80%, the maximum pressure was found to be increasing from 104006 Pa to 106879 Pa, while the minimum pressure inside the pipeline decreased notably from 97176.8 Pa to 94894 Pa. Also, while the inlet pressure varied in the same manner as the maximum pressure, slow initially and steeper afterwards, from 103854.57 Pa to 106616.97 Pa, the outlet pressure fell minorly during the process, from 99592.93 Pa to 98493.91 Pa. The value of pressure drop was found to be ranging between 4261.64 Pa and 8123.06 Pa, or 4.1% to 7.61%. While the pressure at bend 1 of the pipeline system were found to be increasing rapidly, the same for bend 4 was found to be falling albeit slowly, while the same in bends 2 and 3 were found to be decreasing, though for bend 2, it decreased slowly and for bend 3 it decreased rapidly after 70% solids concentration, with an increase in concentration of solid particles in slurry.

4) Variation of Pressure Drop with Varying Diameter of Cross Section of Pipeline

The variations of the diameter of cross section of the pipeline were done by keeping the bend angles of the pipe constant at 6º, and inlet velocity of slurry constant at 1.5 m/s. The inner diameter of the pipeline in all the cases was also maintained at 0.5 inches less than the outer diameter. The diameter of cross section of the pipeline were varied as follows – 10 inches, 15 inches, 20 inches, 25 inches, 30 inches, 35 inches respectively. The radius of curvature of pipeline bend was also kept constant at R2000. The results thus obtained are shown in Table 16 below, and also plotted in graphs.

Table 16 – Variation of pressure inside the pipe with an increase in diameter of cross section of pipe

Diameter of the pipeline (in Inches)	Pressure values in the pipeline (in Pa)								
	Maximum Pressure	Minimum Pressure	Pressure at the Inlet	Pressure at the Outlet	Pressure Drop	Pressure at Bend 1	Pressure at Bend 2	Pressure at Bend 3	Pressure at Bend 4
10	105096	96599.3	104989.44	99594.55	5394.89	102727.68	99277.03	98887.45	101752.45
15	105452	95347.9	105244.13	98646.31	6597.82	102426.83	98945.18	98761.14	101566.14
20	106237	94177.3	105927.63	97655.11	8272.52	102112.6	98613.01	98602.52	101522.95
25	107181	93026	106755.45	96620.55	10134.9	101835.1	98499.44	98556.93	101495.06
30	108178	91915	107676.07	95568.69	12107.38	101747.66	98352.53	98393.53	101400.96
35	109203	90818.7	108631.44	94592.84	14038.6	101502.77	98158.68	98205.71	101212.43

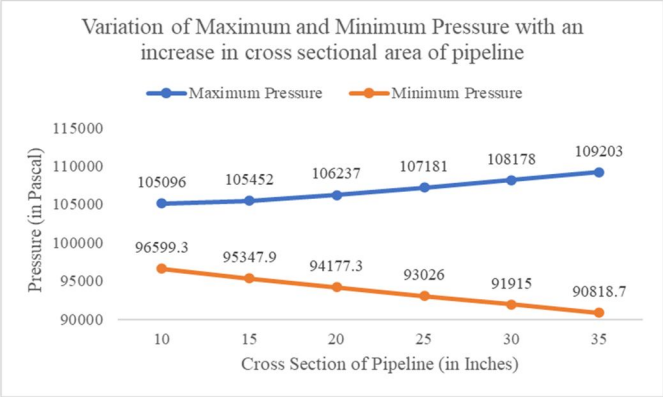

Fig. 52 – Variation of maximum and minimum pressure inside the pipe with increase in diameter of cross section of the pipeline

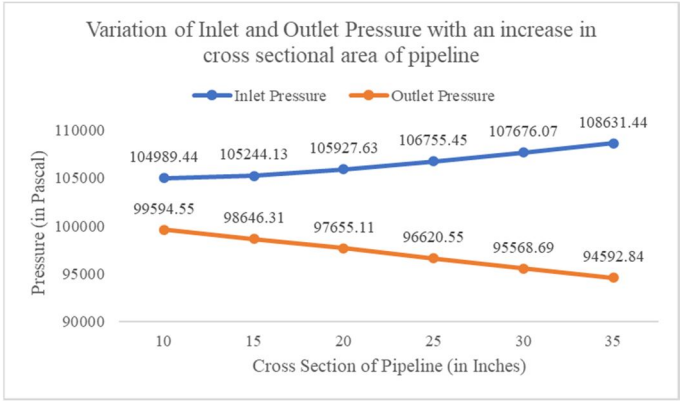

Fig. 53 – Variation of inlet and outlet pressure inside the pipeline with an increase in the diameter of cross section of the pipeline

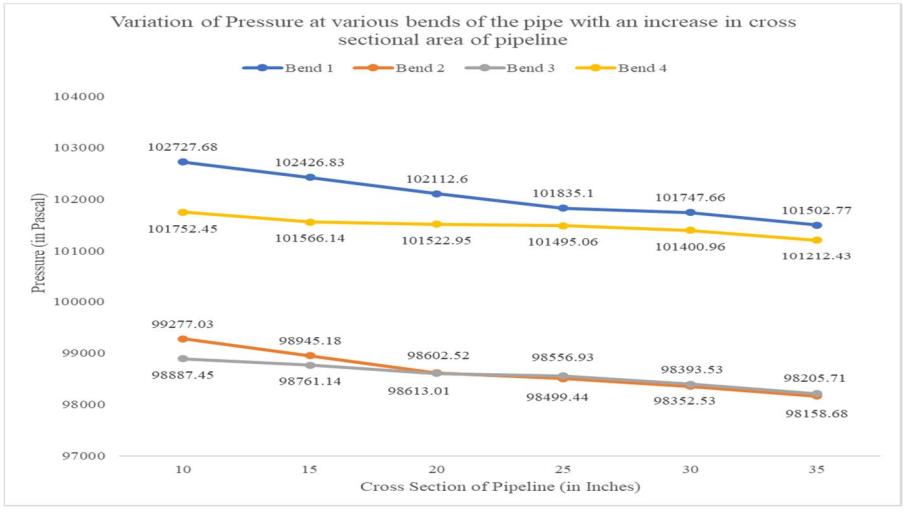

Fig. 54 – Variation pressure at various bends inside the pipe with an increase in diameter of cross section of pipeline

The graphs represented in fig. 52, fig. 53 and fig. 54 indicate the plot of maximum and minimum pressure inside the pipeline vs. diameter of cross section of the pipeline, pressure at the inlet and outlet of the pipe vs. diameter of cross section of the pipeline, and the pressure at various bents of the pipeline with respect to the diameter of cross section of the pipeline, respectively, which were plotted taking into consideration the values obtained from table 16. The observations made are – an increase in the size of the pipeline diameter from 10 inches to 35 inches caused the maximum velocity inside the pipeline to rise substantially from 105096 Pa to 109203 Pa, and the minimum pressure inside the pipeline to fall steeply from 96599.3 Pa to 90818.7 Pa. The pressure at the inlet of the pipeline rose notably from 104989.44 Pa to 108631.44 Pa, and the outlet pressure fell substantially from 99594.5 Pa to 94592.84 Pa. The value of pressure drop was found to be ranging between 5394.89 Pa and 14038.6 Pa, or 5.13% to 12.92%. While the pressure at all the four bends were found to be decreasing, the pressure values at bends 2, 3 and 4 decreased slowly, the same for bend 1 decreased steeply with an increase in concentration of solid particles in slurry.

E. For Radius of Curvature of Bends – R2500

1) Variation of pressure drop with varying bend angles of the pipeline

The variations of the angles of bends of the pipeline were done by keeping the area of cross section/outer diameter of the pipeline constant at 15 inches, and inlet velocity of slurry constant at 1.5 m/s. The inner diameter of the pipeline in all the cases was also maintained at 14.5 inches. The bend angles were varied as follows - 3°, 6°, 9°, 12°, 15°, and 18°, respectively. The radius of curvature of pipeline bend was also kept constant at R2500. The results thus obtained are shown in Table 17 below, and also plotted in graphs.

Table 17 – Variation of pressure inside the pipeline with an increase in bend angles

Bend Angles (in °)	Pressure values in the pipeline (in Pa)								
	Maximum Pressure	Minimum Pressure	Pressure at the Inlet	Pressure at the Outlet	Pressure Drop	Pressure at Bend 1	Pressure at Bend 2	Pressure at Bend 3	Pressure at Bend 4
3	105297	97300.6	103790.29	100167.43	3622.86	101528.18	100128.17	100748.23	102525.8
6	105318	95548.4	103879.77	100128.41	3751.66	101631.3	98940.22	98568.75	101883.11
9	105349	93796.9	105105.7	98892.09	6213.61	101674.12	97490.43	97170.27	101562.12
12	105370	92062	105195.13	98771.72	6423.41	101767.34	95323.95	96055.15	101292.17
15	105374	90355.7	105225.36	98720.85	6504.51	102023.69	94295.03	94043.81	101080.81
18	105388	88672	105232.27	98703.27	6529	102632.18	92558.86	92632.2	101050.98

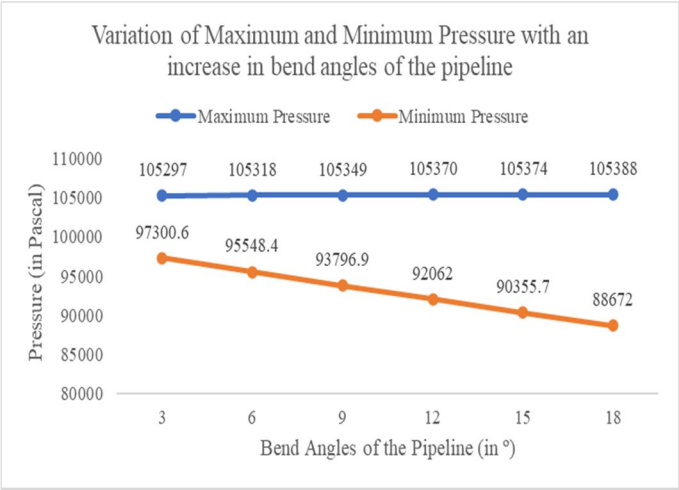

Fig. 55 – Variation of maximum and minimum pressure inside the pipe with increase in bend angles of the pipe

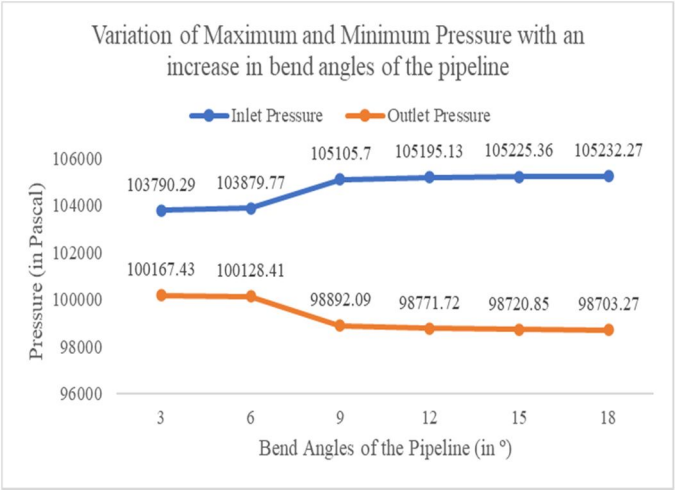

Fig. 56 – Variation of inlet and outlet pressure inside the pipeline with an increase in the bend angles of the pipe

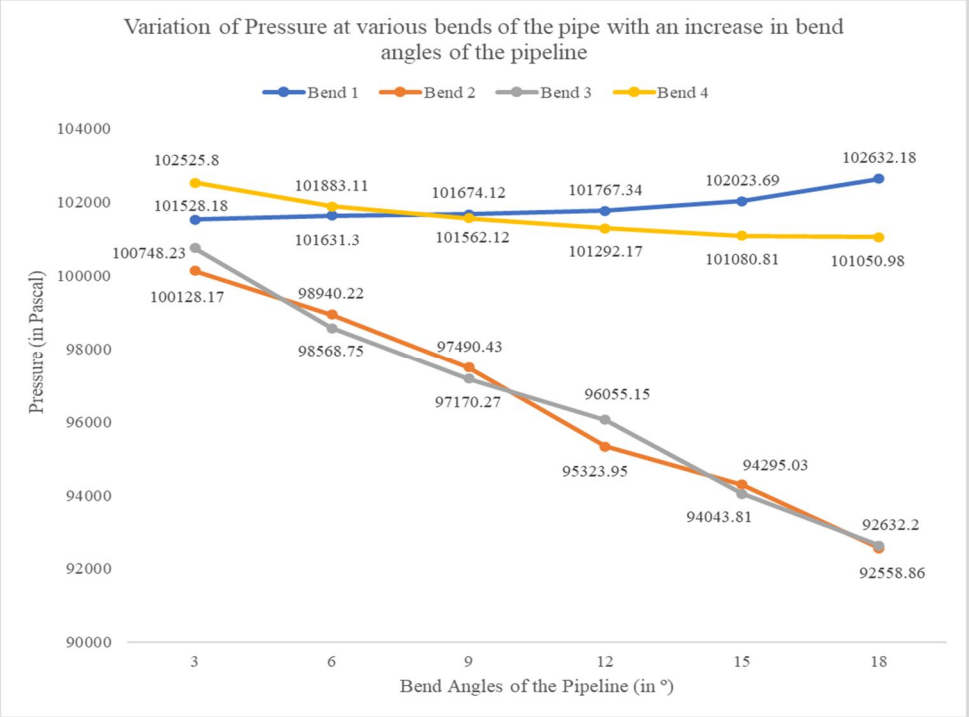

Fig. 57 – Variation pressure at various bends inside the pipeline with an increase in the bend angles of the pipe

The graphs represented in fig. 55, fig. 56 and fig. 57 indicate the plot of maximum and minimum pressure inside the pipeline vs. bend angles of the pipe system, pressure at the inlet and outlet of the pipe vs. bend angles of the pipe system, and the pressure at various bents of the pipeline with respect to the bend angles, respectively, which were plotted taking into consideration the values obtained from table 17. The observations made are – with an increase in angle of bend of the pipeline system from 3º to 18º, the maximum pressure increased marginally from 105297 Pa to 105388 Pa, and the minimum pressure dropped substantially from 97300.6 Pa to 88672 Pa. But the pressure at the inlet somewhat noticeably increased, from 103790.29 Pa to 105232.27 Pa and the outlet pressure decreased in a similar fashion from 100167.43 Pa to 98703.27 Pa respectively. The value of pressure drop was found to be ranging between 3622.86 Pa and 6529 Pa, or 3.49% to 6.2%. While the pressure at bend 1 of the pipeline system was found to be increasing, pressure at bend 4 dropped minorly, while the same in bends 2 and 3 were found to be decreasing substantially with an increase in the angles of bend of the pipeline.

2) Variation of Pressure drop with varying inlet Velocity of Slurry

The variations of the inlet velocity of slurry were done by keeping the area of cross section/outer diameter of the pipeline constant at 15 inches, and bend angles at 6º. The inner diameter of the pipeline in all the cases was also maintained at 14.5 inches. The inlet velocities were varied as follows – 0.5 m/s, 1.0 m/s, 1.5 m/s, 2.0 m/s, 2.5 m/s, and 3.0 m/s respectively. The radius of curvature of pipeline bend was also kept constant at R2500. The results thus obtained are shown in Table 18 below, and also plotted in graphs.

Table 18 – Variation of pressure inside the pipeline with an increase in inlet velocity of slurry

Inlet Velocity (in m/s)	Pressure values in the pipeline (in Pa)								
	Maximum Pressure	Minimum Pressure	Pressure at the Inlet	Pressure at the Outlet	Pressure Drop	Pressure at Bend 1	Pressure at Bend 2	Pressure at Bend 3	Pressure at Bend 4
0.5	104305	95236.3	104126.62	98867.11	5259.51	101408.58	98399.79	98349.52	101287.87
1.0	104704	95369.5	104493.93	98887.12	5606.81	101649.53	98595.38	98456.16	101317.37
1.5	105335	95584.8	105154.99	98890.87	6264.12	102068.62	98831.66	98608.73	101478.1
2.0	106182	95885	105966.65	98892.77	7073.88	102880.87	99328.94	98883.54	101528.04
2.5	107233	96252.8	107007.87	98894.61	8113.26	103681.7	99888.22	99209.59	101621.71
3.0	108981	96691.4	108249.82	98900.86	9348.96	104771.78	101090.03	99674.53	101979.87

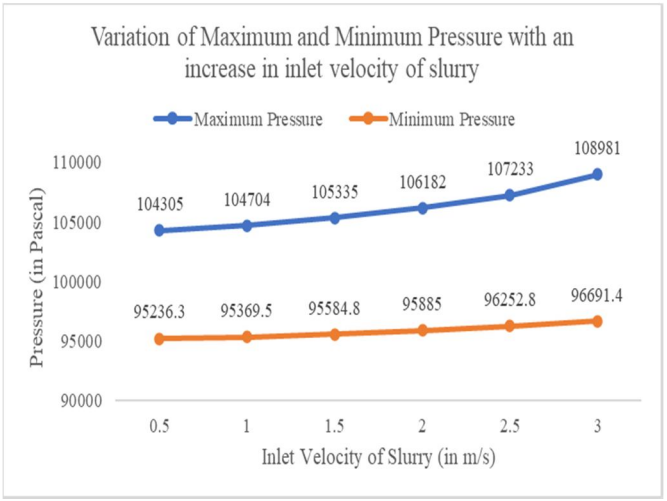

Fig. 58 – Variation of maximum and minimum pressure inside the pipe with increase in inlet velocity of slurry

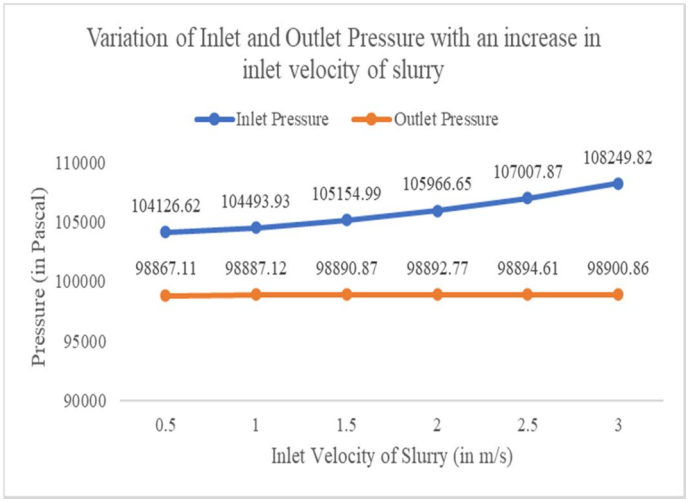

Fig. 59 – Variation of inlet and outlet pressure inside the pipeline with an increase in the inlet velocity of slurry

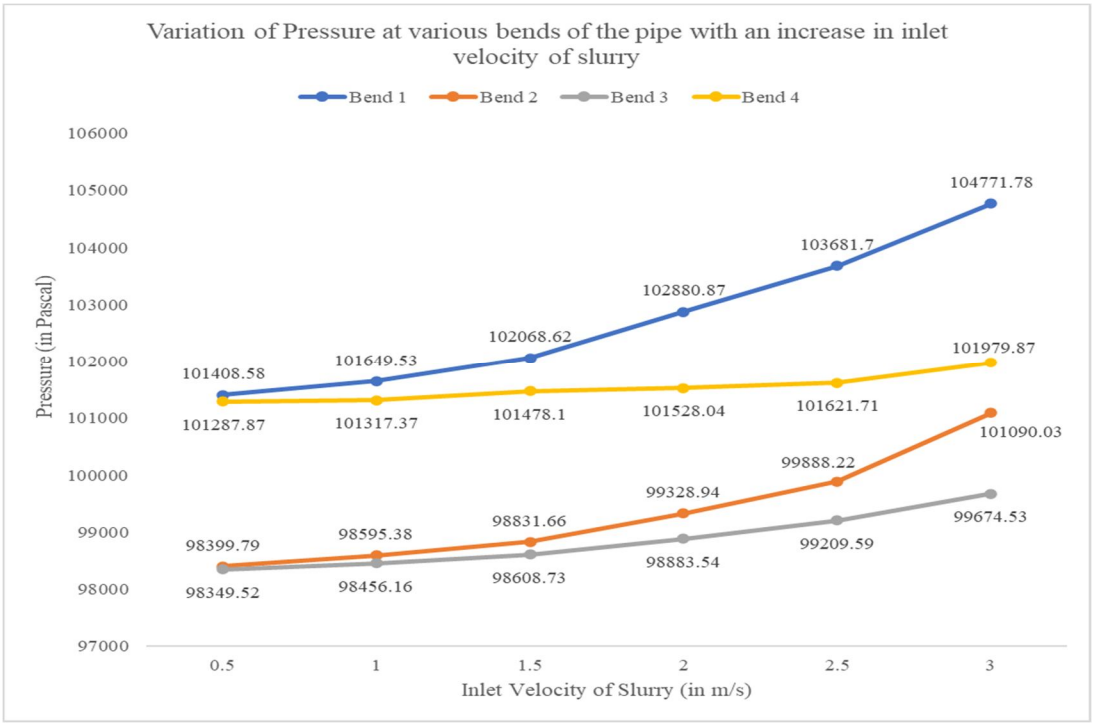

Fig. 60 – Variation pressure at various bends inside the pipeline with an increase in the inlet velocity of slurry

The graphs represented in fig. 58, fig. 59 and fig. 60 indicate the plot of maximum and minimum pressure inside the pipeline vs. inlet velocity of slurry, pressure at the inlet and outlet of the pipe vs. inlet velocity of slurry, and the pressure at various bents of the pipeline with respect to the inlet velocity of slurry, respectively, which were plotted taking into consideration the values obtained from table 18. The observations made are – with an increase in velocity at the inlet of the pipeline system from 0.5 m/s to 3 m/s, the maximum pressure increased substantially from 104305 Pa to 108981 Pa, and the minimum pressure increased minorly from 95236.3 Pa to 96691.4 Pa. The pressure at the inlet increased during the process, albeit the rise in pressure at the inlet was steep, i.e., from 104126.62 Pa to 108249.82 Pa, as compared to the marginal rise in pressure at the outlet of the pipe, i.e., from 98867.1 Pa to 98900.86 Pa. The value of pressure drop was found to be ranging between 5259.51 Pa and 9348.96 Pa, or 5.05% to 8.63%. The pressure at bends at all the 4 bends were found to be increasing with an increase in the inlet velocity of slurry. While pressure at bend 1 increased rapidly, the same for bends 2 and 3 increased substantially, while for bend 4, it increased marginally.

3) Variation of Pressure Drop with Varying Concentration of Solid Particles in Slurry

The variations of the concentration of solids in slurry were done by keeping the area of cross section/outer diameter of the pipeline constant at 15 inches, and inlet velocity of slurry constant at 1.5 m/s. The inner diameter of the pipeline in all the cases was also maintained at 14.5 inches. The concentration of solids in slurry were varied as follows – 30%, 40%, 50%, 60%, 70% and 80% respectively. The radius of curvature of pipeline bend was also kept constant at R2500. The results thus obtained are shown in Table 19 below, and also plotted in graphs.

Table 19 – Variation of pressure inside the pipe with an increase in concentration of solids in slurry

Concentration of solids in slurry (in %)	Pressure values in the pipeline (in Pa)								
	Maximum Pressure	Minimum Pressure	Pressure at the Inlet	Pressure at the Outlet	Pressure Drop	Pressure at Bend 1	Pressure at Bend 2	Pressure at Bend 3	Pressure at Bend 4
30	104001	97173.1	103849.99	99589.78	4260.21	101746.04	99441.24	99418.6	101476.68
40	104263	96816	104100.54	99443.99	4656.55	101897.75	99242.82	99354.7	101575.01
50	104563	96438.4	104410.93	99269.01	5141.92	102097.46	99229.82	99223.33	101645.24
60	104952	95962.7	104754.85	99063.68	5691.17	102142.35	99200.13	99023.95	101690.43
70	105567	95422.5	105347.27	98809.67	6537.6	102525.89	99181.86	98489.16	101764.6
80	106875	94899	106619.02	98491.75	8127.27	103124.8	99143.2	98476.07	101952.24

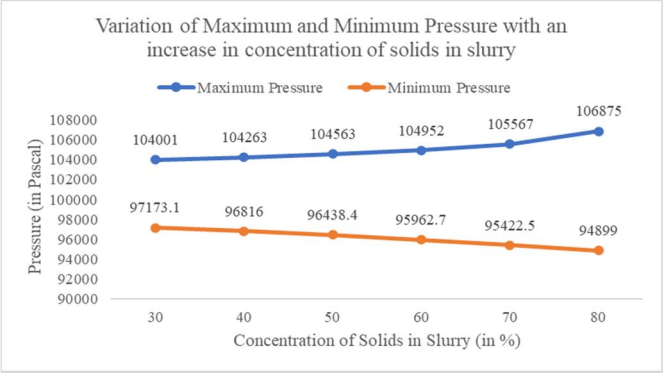

Fig. 61 – Variation of maximum and minimum pressure inside the pipe with increase in concentration of solids in slurry

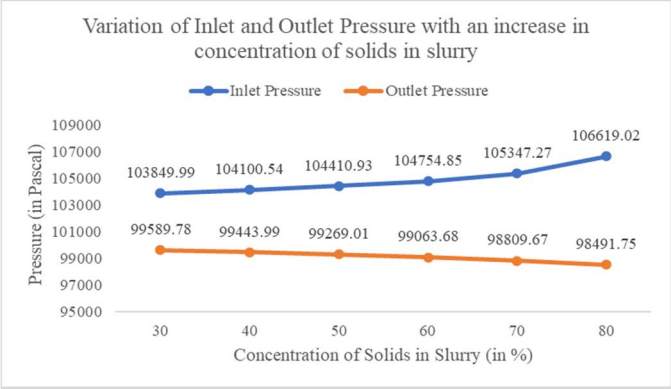

Fig. 62 – Variation of inlet and outlet pressure inside the pipeline with an increase in the concentration of solids in slurry

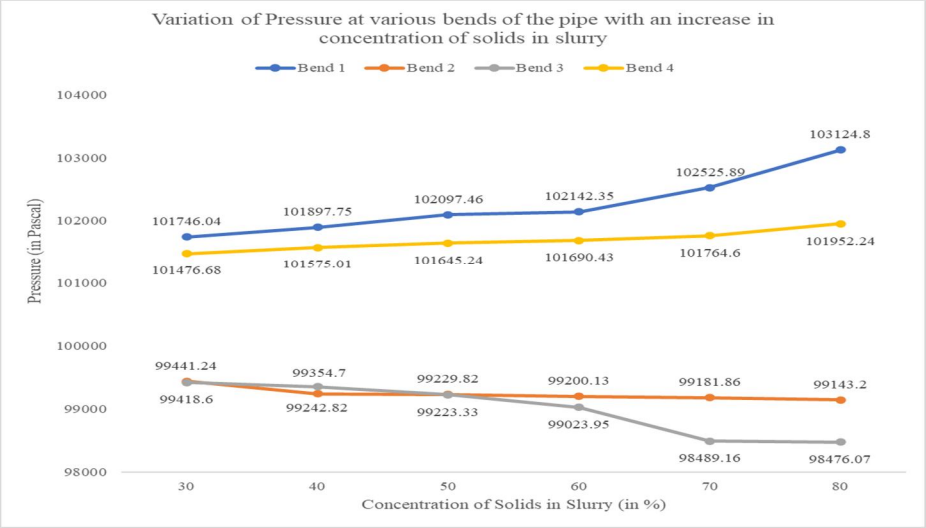

Fig. 63 – Variation pressure at various bends inside the pipeline with an increase in concentration of solids in slurry

The graphs represented in fig. 61, fig. 62 and fig. 63 indicate the plot of maximum and minimum pressure inside the pipeline vs. concentration of solids in slurry, pressure at the inlet and outlet of the pipe vs. concentration of solids in slurry, and the pressure at various bents of the pipeline with respect to the concentration of solids in slurry, respectively, which were plotted taking into consideration the values obtained from table 19. The observations made are – when the concentration of solids in the slurry flowing inside the pipeline was increased from 30% to 80%, the maximum pressure was found to be increasing from 104001 Pa to 106875 Pa, while the minimum pressure inside the pipeline decreased notably from 97173.1 Pa to 94899 Pa. Also, while the inlet pressure varied in the same manner as the maximum pressure, slow initially and steeper afterwards, from 103849.99 Pa to 106619.02 Pa, the outlet pressure fell minorly during the process, from 99589.78 Pa to 98491.75 Pa. The value of pressure drop was found to be ranging between 4260.21 Pa and 8127.27 Pa, or 4.1% to 7.62%. While the pressure at bend 1 of the pipeline system were found to be increasing rapidly, the same for bend 4 was found to be falling albeit slowly, while the same in bends 2 and 3 were found to be decreasing, though for bend 2, it decreased slowly and for bend 3 it decreased rapidly after 60% solids concentration, with an increase in concentration of solid particles in slurry.

4) Variation of Pressure drop with Varying Diameter of cross Section of Pipeline

The variations of the diameter of cross section of the pipeline were done by keeping the bend angles of the pipe constant at 6º, and inlet velocity of slurry constant at 1.5 m/s. The inner diameter of the pipeline in all the cases was also maintained at 0.5 inches less than the outer diameter. The diameter of cross section of the pipeline were varied as follows – 10 inches, 15 inches, 20 inches, 25 inches, 30 inches, 35 inches respectively. The radius of curvature of pipeline bend was also kept constant at R2500. The results thus obtained are shown in Table 20 below, and also plotted in graphs.

Table 20 – Variation of pressure inside the pipe with an increase in diameter of cross section of pipe

Diameter of the pipeline (in Inches)	Pressure values in the pipeline (in Pa)								
	Maximum Pressure	Minimum Pressure	Pressure at the Inlet	Pressure at the Outlet	Pressure Drop	Pressure at Bend 1	Pressure at Bend 2	Pressure at Bend 3	Pressure at Bend 4
10	105096	96601.1	104989.13	99594.43	5394.7	102885.97	99371.11	98803.29	101528.41
15	105450	95345.1	105239.92	98645.32	6594.6	102309.26	98983.52	98474.52	101443.98
20	106198	94175	105912.02	97655.11	8256.91	102123.74	98887.74	98459.71	101185.99
25	107150	93023.7	106741.05	96620.88	10120.17	101583.73	98663.44	98391.57	101128.98
30	108140	91908.3	107664.82	95560.45	12104.37	101502.62	98628.66	98358.24	101100.13
35	109171	90810.2	108613.45	94587.77	14025.68	101487.47	98578.56	98292.29	100926.95

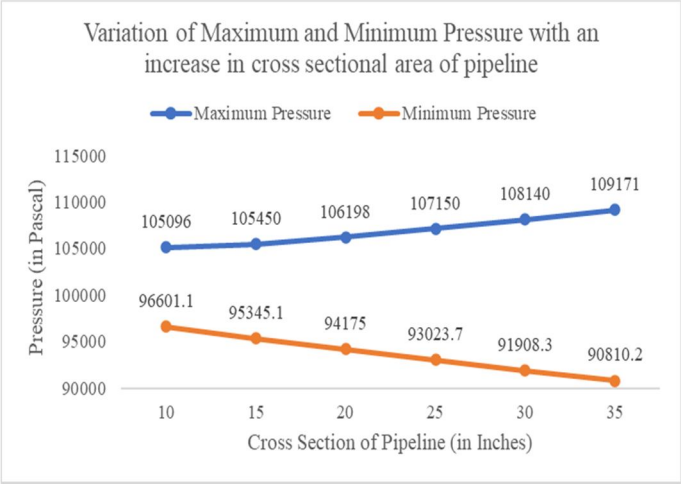

Fig. 64 – Variation of maximum and minimum pressure inside the pipe with increase in diameter of cross section of the pipeline

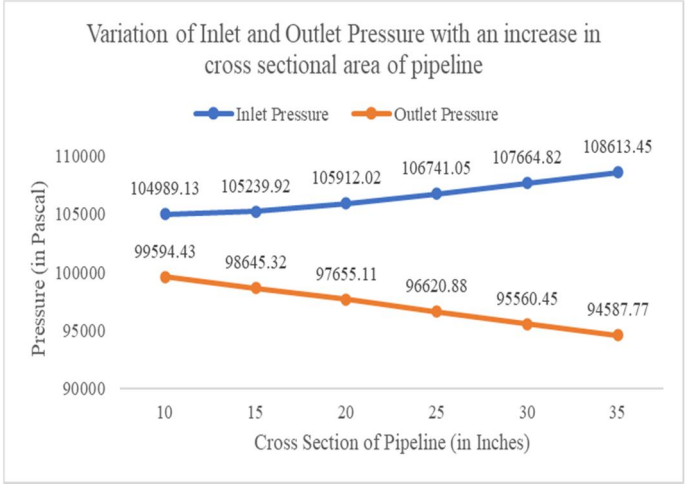

Fig. 65 – Variation of inlet and outlet pressure inside the pipeline with an increase in the diameter of cross section of the pipeline

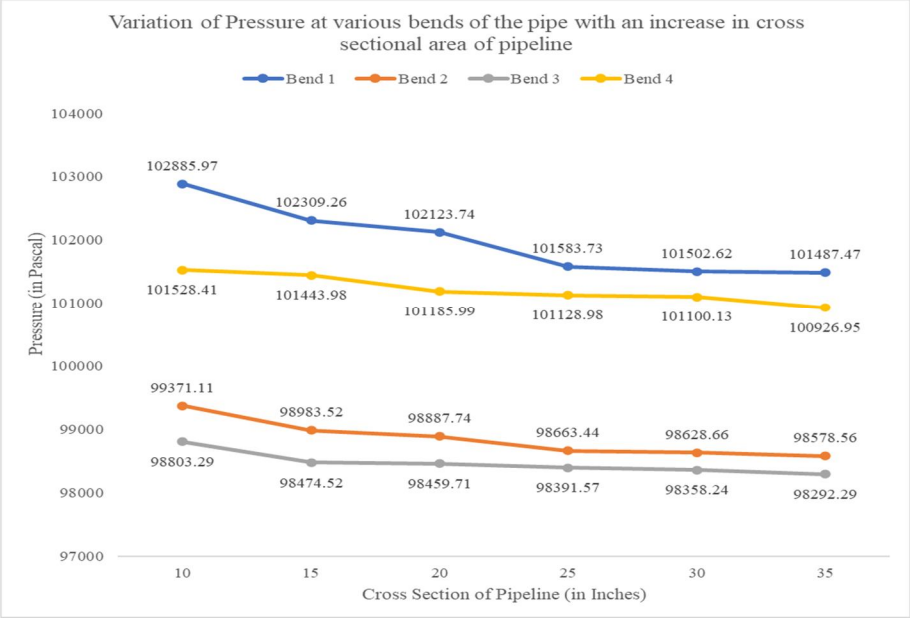

Fig. 66 – Variation pressure at various bends inside the pipe with an increase in diameter of cross section of pipeline

The graphs represented in fig. 64, fig. 65 and fig. 66 indicate the plot of maximum and minimum pressure inside the pipeline vs. diameter of cross section of the pipeline, pressure at the inlet and outlet of the pipe vs. diameter of cross section of the pipeline, and the pressure at various bents of the pipeline with respect to the diameter of cross section of the pipeline, respectively, which were plotted taking into consideration the values obtained from table 20. The observations made are – an increase in the size of the pipeline diameter from 10 inches to 35 inches caused the maximum velocity inside the pipeline to rise substantially from 105096 Pa to 109171 Pa, and the minimum pressure inside the pipeline to fall steeply from 96601.1 Pa to 90810.2 Pa. The pressure at the inlet of the pipeline rose notably from 104989.13 Pa to 108613.45 Pa, and the outlet pressure fell substantially from 99594.43 Pa to 94587.77 Pa. The value of pressure drop was found to be ranging between 5394.7 Pa and 14025.68 Pa, or 5.13% to 12.91%. While the pressure at all the four bends were found to be decreasing, the pressure values at bends 2, 3 and 4 decreased slowly, the same for bend 1 decreased steeply with an increase in concentration of solid particles in slurry.

VI. CONCLUSION AND FUTURE SCOPE

Comparatively a newer technique, pipeline transportation of slurry is widely used considering the several advantages it has over bulk transportation by the means of rail, road and port. Nowadays, many researchers have shown their interest and have experimented with the design of hydraulic transport systems. Several researchers have also established many mathematical relations and numerical models relating various flow parameters. Pressure drop is among the major challenges needed to be tackled by transportation plants, for it contributes to a decreased efficiency and increased loss of power, time as well as is not economical. This article investigated upon the pressure drop inside the slurry pipelines under various circumstances, under different sets of operating conditions. The overall pressure drop under these varying conditions, was found out to be lying between 3.41%-12.91%. After the calculations and plotting of graphs were done, the detailed results thus obtained were –

1) With an increase in the angles of bend of the piping system, for the case of all radius of bends of the pipeline, the maximum pressure inside the pipeline was found to be increasing marginally, but the minimum pressure fell noticeably. When compared, it was noticed that, for higher values of radius of curvature of bend, both the maximum and minimum pressure were decreasing. The inlet pressure, in all cases of radius of curvatures of bends, was found to be increasing slowly till a bend angle of 6°, after which, it increased substantially. Similarly, the outlet pressure, in all cases of radius of curvatures of bends, was found to be decreasing slowly till a bend angle of 6°, after which, it decreased substantially. The pressure drop for R500 radius of curvature of bends was found to be lying between 4438.21 Pa to 6900.92 Pa, i.e., 4.27% to 6.53%, as the bend angles increased from 3° to 18°, while the same was found to be lying between 3622.86 Pa to 6529 Pa, i.e., 3.49% to 6.2% for R2500 radius of curvature of bends. A trend of decreasing pressure drop was observed with an increase in radius of curvature of bends, which shows that a lower value of bend angle, combined with higher value of radius of curvature of bend is suitable for pipelines.

2) With an increase in the velocity at the inlet of the pipeline, maximum pressure inside the pipeline was found to be increasing substantially, while the minimum pressure inside the pipeline was found to be increasing minorly and this trend was observed for all the values of radius of curvature of bends. Both the pressures at the inlet and the outlet increased during the process, albeit the rise in pressure at the inlet was steep as compared to the marginal rise in pressure at the outlet in all cases of radius of curvature of bends. The pressure drop for R500 radius of curvature of bends was found to be lying between 5109.59 Pa to 8965.22 Pa, i.e., 4.91% to 8.3%, as the inlet velocity of slurry increased from 0.5 m/s to 3m/s, while the same was found to be lying between 5259.51 Pa to 9348.96 Pa, i.e., 5.05% to 8.63% for R2500 radius of curvature of bends. As the radius of curvature of bends were increased, the pressure drop remained same, more or less, as the increase was minor, which shows that a combination of higher value of radius of curvature of bend and lower inlet velocity of slurry can be preferable, subject to condition that the inlet velocity of slurry is well above the settling velocity.

3) When the concentration of solids in the slurry flowing inside the pipeline was increased, the maximum pressure was found to be increasing marginally initially, and later on, the rise was substantial, while the minimum pressure inside the pipeline notably decreased for all cases of radius of curvature of bends. Similarly, it was noteworthy that while the inlet pressure varied in the same manner as the maximum pressure, slow initially and steeper afterwards, the outlet pressure fell minorly during the process in all cases of radius of curvatures of bends. The pressure drop for R500 radius of curvature of bends was found to be lying between 4281.22 Pa to 8167.01 Pa, i.e., 4.12% to 7.65%, as the concentration of solids in slurry increased from 30% to 80%, while the same was found to be lying between 4260.21 Pa to 8127.27 Pa, i.e., 4.09% to 7.62% for R2500 radius of curvature of bends. As the radius of curvature of bends were increased, the pressure drop value remained the same, more or less, as the decrease in pressure drop values with increase in radius of curvature of bends was relatively minor, which shows that a combination of higher value of radius of curvature of bend and lower concentration of solids in slurry would be preferable considering the fact that as the radius of curvature of bends of the pipeline increase, the maximum pressure inside the pipeline reduces.

4) An increase in the diameter of the pipeline, which had a uniform circular cross section, caused the maximum pressure in the pipeline to rise substantially and the minimum pressure to fall steeply. The same was also observed with the pressures at the inlet and outlet. While the inlet pressure rose, the pressure at the outlet saw a steep decline. The pressure drop for R500 radius of curvature of bends was found to be lying between 5414.88 Pa to 14031.77 Pa, i.e., 5.15% to 12.91%, as the diameter of cross section of the pipeline increased from 10 inches to 35 inches, while the same was found to be lying between 5394.7 Pa to 14025.68 Pa, i.e., 5.13% to 12.91% for R2500 radius of curvature of bends. As the radius of curvature of bends were increased, the pressure drop value remained the same, more or less, as the decrease in pressure drop values with increase in radius of curvature of bends was relatively minor, which shows that a combination of higher value of radius of curvature of bend and lower diameter of cross section of pipe would be preferable considering the fact that as the radius of curvature of bends of the pipeline increase, the maximum pressure inside the pipeline reduces. Though, for higher carrying capacity, higher diameter of cross section would be required, and for that purpose, the other parameters such as slurry inlet velocity and concentration of solids in slurry need to be altered suitably to keep the pressure drop value in check.

Slurry being a two-phase liquid, its modelling and flow simulation as well as its actual transportation is a critical task considering the involvement of several parameters, variables, laws of physics, numerical models and mathematical equations. The chemical composition of slurry, the varying mineralogy of ores has an effect on the rheology of slurry and also affects the flow which can be a possible research field. Back flow issues, bends, changes in elevation profile and improvement of the ore of various grades are also possible areas where investigation can be carried out. The transportation of slurry via pipelines proves to be beneficial in several terms, but also along with that, it opens the doors for further research and optimization of the same.

A. Nomenclature

D	Diameter of the pipeline
τ_W	Shear stress at the pipe wall
P_1 & P_2	Pressures at sections 1 and 2
L	Distance between sections 1 and 2
ρ	Density of the fluid
U	Average velocity of flow
C_w	Concentration of solids in percent by weight

ρ_s	Density of solid
ρ_l	Density of liquid
ρ_f	Slurry density
g	Acceleration due to gravity
ρ_M	Specific gravity of the suspending medium
S, or, S_s	Ratio of the density of solids to the density of the slurry
μ_w	Water dynamic viscosity, or, Saturated water absolute viscosity at t=32ºC
ρ_S	Solid's specific gravity
C_v	Volume percent solids
d	Particle diameter
μ_f	Slurry dynamic viscosity
V_c, or, V_D	Critical deposition velocity
Fr	Froude's number
Ar	Archimedes number

REFERENCES

[1] Singh, J., & Singh, J. P. (2021). Numerical analysis on solid particle erosion in elbow of a slurry conveying circuit. Journal of Pipeline Systems Engineering and Practice, 12(1), 04020070.
[2] Brown, G. (2006, December). Use of CFD to predict and reduce erosion in an industrial slurry piping system. In Fifth International Conference on CFD in the process industries. CSIRO, Melbourne, Australia (pp. 13-15).
[3] Singh, J. P., Kumar, S., & Mohapatra, S. K. (2021). Simulation and optimization of coal-water slurry suspension flow through 90° pipe bend using CFD. International Journal of Coal Preparation and Utilization, 41(6), 428-450.
[4] Azimian, M., & Bart, H. J. (2014). Investigation of hydroabrasion in slurry pipeline elbows and T-junctions. Journal of Energy and Power Engineering, 8(1), 65.
[5] TURIAN, R. M., Hsu, F. L., & Selim, M. S. (1983). Friction losses for flow of slurries in pipeline bends, fittings, and valves. Particulate Science and Technology, 1(4), 365-392.
[6] Kumar, A., Kaushal, D. R., & Kumar, U. (2008). Bend pressure drop experiments compared with FLUENT. Proceedings of the Institution of Civil Engineers-Engineering and Computational Mechanics, 161(1), 35-42.
[7] Mishra, R., Singh, S. N., & Seshadri, V. (1998). Pressure drop across conventional and diverging-converging pipe bends in the flow of multi-sized particulate slurries.
[8] Verma, A. K., Singh, S. N., & Seshadri, V. (2006). Pressure drop for the flow of high concentration solid-liquid mixture across 90º horizontal conventional circular pipe bend.
[9] Zhang, J., Kang, J., Fan, J., & Gao, J. (2016). Research on erosion wear of high-pressure pipes during hydraulic fracturing slurry flow. Journal of Loss Prevention in the Process Industries, 43, 438-448.
[10] Peng, W., & Cao, X. (2016). Numerical simulation of solid particle erosion in pipe bends for liquid–solid flow. Powder technology, 294, 266-279.
[11] Wood, R. J. K., Jones, T. F., Ganeshalingam, J., & Miles, N. J. (2004). Comparison of predicted and experimental erosion estimates in slurry ducts. Wear, 256(9-10), 937-947.
[12] Singh, V., Kumar, S., & Mohapatra, S. K. (2019). Modeling of erosion wear of sand water slurry flow through pipe bend using CFD. Journal of Applied Fluid Mechanics, 12(3), 679-687.
[13] Rawat, K. S., Verma, A., Uniyal, A., Gangwar, H. P., & Pratihar, A. K. (2020, March). Modeling of Ice Slurry Flow through Bend Pipe. In IOP Conference Series: Materials Science and Engineering (Vol. 802, No. 1, p. 012001). IOP Publishing.
[14] Wood, R. J. K., Jones, T. F., Miles, N. J., & Ganeshalingam, J. (2001). Upstream swirl-induction for reduction of erosion damage from slurries in pipeline bends. Wear, 250(1-12), 770-778.
[15] Kannojiya, V., & Kumar, S. (2020). Assessment of optimum slurry pipe design for minimum erosion. Scientia Iranica, 27(5), 2409-2418.
[16] Doron, P., & Barnea, D. (1995). Pressure drop and limit deposit velocity for solid-liquid flow in pipes. Chemical engineering science, 50(10), 1595-1604.
[17] Doron, P., Granica, D., & Barnea, D. (1987). Slurry flow in horizontal pipes—experimental and modeling. International journal of multiphase flow, 13(4), 535-547.
[18] Verma, O. P., Kumar, A., & Sikarwar, B. S. (2020). Numerical simulation and comparative analysis of pressure drop estimation in horizontal and vertical slurry pipeline. Journal of Mechanical Engineering and Sciences, 14(2), 6610-6624.
[19] Singh, M. K., Kumar, S., & Ratha, D. (2020). Computational analysis on disposal of coal slurry at high solid concentrations through slurry pipeline. International Journal of Coal Preparation and Utilization, 40(2), 116-130.
[20] Kaushal, D. R., & Tomita, Y. (2002). An improved method for predicting pressure drop along slurry pipeline. Particulate science and technology, 20(4), 305-324.
[21] Chandel, S., Seshadri, V., & Singh, S. N. (2009). Effect of additive on pressure drop and rheological characteristics of fly ash slurry at high concentration. Particulate Science and Technology, 27(3), 271-284.
[22] Turian, R. M., & Yuan, T. F. (1977). Flow of slurries in pipelines. AIChE Journal, 23(3), 232-243.
[23] Sanders, R. S., Schaan, J., Hughes, R., & Shook, C. (2004). Performance of sand slurry pipelines in the oil sands industry. The Canadian Journal of Chemical Engineering, 82(4), 850-857.

[24] Herna´ ndez, F. H., Blanco, A. J., & Rojas-Solo´ rzano, L. (2008, January). CFD modeling of slurry flows in horizontal pipes. In Fluids Engineering Division Summer Meeting (Vol. 48401, pp. 857-863).
[25] Ekambara, K., Sanders, R. S., Nandakumar, K., & Masliyah, J. H. (2009). Hydrodynamic simulation of horizontal slurry pipeline flow using ANSYS-CFX. Industrial & Engineering Chemistry Research, 48(17), 8159-8171.
[26] Kaushal, D. R., Thinglas, T., Tomita, Y., Kuchii, S., & Tsukamoto, H. (2012). CFD modeling for pipeline flow of fine particles at high concentration. International Journal of Multiphase Flow, 43, 85-100.
[27] Wu, D., Yang, B., & Liu, Y. (2015). Pressure drop in loop pipe flow of fresh cemented coal gangue–fly ash slurry: Experiment and simulation. Advanced Powder Technology, 26(3), 920-927.
[28] Wang, J., Wang, S., Zhang, T., & Battaglia, F. (2017). Mathematical and experimental investigation on pressure drop of heterogeneous ice slurry flow in horizontal pipes. International Journal of Heat and Mass Transfer, 108, 2381-2392.
[29] Kaushal, D. R., Sato, K., Toyota, T., Funatsu, K., & Tomita, Y. (2005). Effect of particle size distribution on pressure drop and concentration profile in pipeline flow of highly concentrated slurry. International Journal of Multiphase Flow, 31(7), 809-823.
[30] Monteiro, A. C., & Bansal, P. K. (2010). Pressure drop characteristics and rheological modeling of ice slurry flow in pipes. International journal of refrigeration, 33(8), 1523-1532.
[31] Li, M. Z., He, Y. P., Liu, Y. D., & Huang, C. (2018). Pressure drop model of high-concentration graded particle transport in pipelines. Ocean Engineering, 163, 630-640.
[32] Matoušek, V. (2009). Predictive model for frictional pressure drop in settling-slurry pipe with stationary deposit. Powder Technology, 192(3), 367-374.
[33] Wang, Z., Kou, Y., Wang, Z., Wu, Z., & Guo, J. (2022). Random Forest Slurry Pressure Loss Model Based on Loop Experiment. Minerals, 12(4), 447.
[34] Kaushal, D. R., & Tomita, Y. (2003). Comparative study of pressure drop in multisized particulate slurry flow through pipe and rectangular duct. International Journal of Multiphase Flow, 29(9), 1473-1487.
[35] Lahiri, S. K., & Ghanta, K. C. (2008). Prediction of pressure drop of slurry flow in pipeline by hybrid support vector regression and genetic algorithm model. Chinese Journal of Chemical Engineering, 16(6), 841-848.
[36] Thomas, D.G., 1964. Periodic phenomena observed with spherical particles in horizontal pipes. Science, 144(3618), pp.534-536.
[37] Thomas, D.G., 1964. Transport characteristics of suspensions: Part IX. Representation of periodic phenomena on a flow regime diagram for dilute suspension transport. AIChE Journal, 10(3), pp.303-308.
[38] Dodge DW and AB Metzner. 1959. “Turbulent Flow of Non-Newtonian Systems.” AIChE Journal 5:189–204.
[39] Durand R and E Condolios. 1952. In Compte Rendu de Deuxiemes Journees de l’Hydraulique, Societe Hydrotechnique de France, Paris pp. 29-55.
[40] Gillies RG, and CA Shook. 1991. “A Deposition Velocity Correlation for Water Slurries.” Canadian Journal of Chemical Engineering 69(5):1225–1228.
[41] Singh, K. P., Kumar, A., & Kaushal, D. R. (2019). CFD modelling and experimental investigation of bimodal slurry flow in horizontal pipeline and bends. In Advances in Fluid and Thermal Engineering (pp. 337-345). Springer, Singapore.
[42] Hoffman, D. M., & McKinley, B. M. (1985). Crystallinity as a selection criterion for engineering properties of high-density polyethylene. Polymer Engineering & Science, 25(9), 562-569.
[43] Burström, P. (2015). Computational Fluid Dynamics of Processes in Iron Ore Grate-kiln Plants (Doctoral dissertation, Luleå tekniska universitet).
[44] Swamy, M., Díez, N. G., & Twerda, A. (2015). Numerical modelling of the slurry flow in pipelines and prediction of flow regimes. WIT Trans Eng Sci, 89(2015), 311-322.
[45] Lahiri, S. K., & Ghanta, K. C. (2009). Study on slurry flow modelling in pipeline. National Institute of Technology, Durgapur, India.

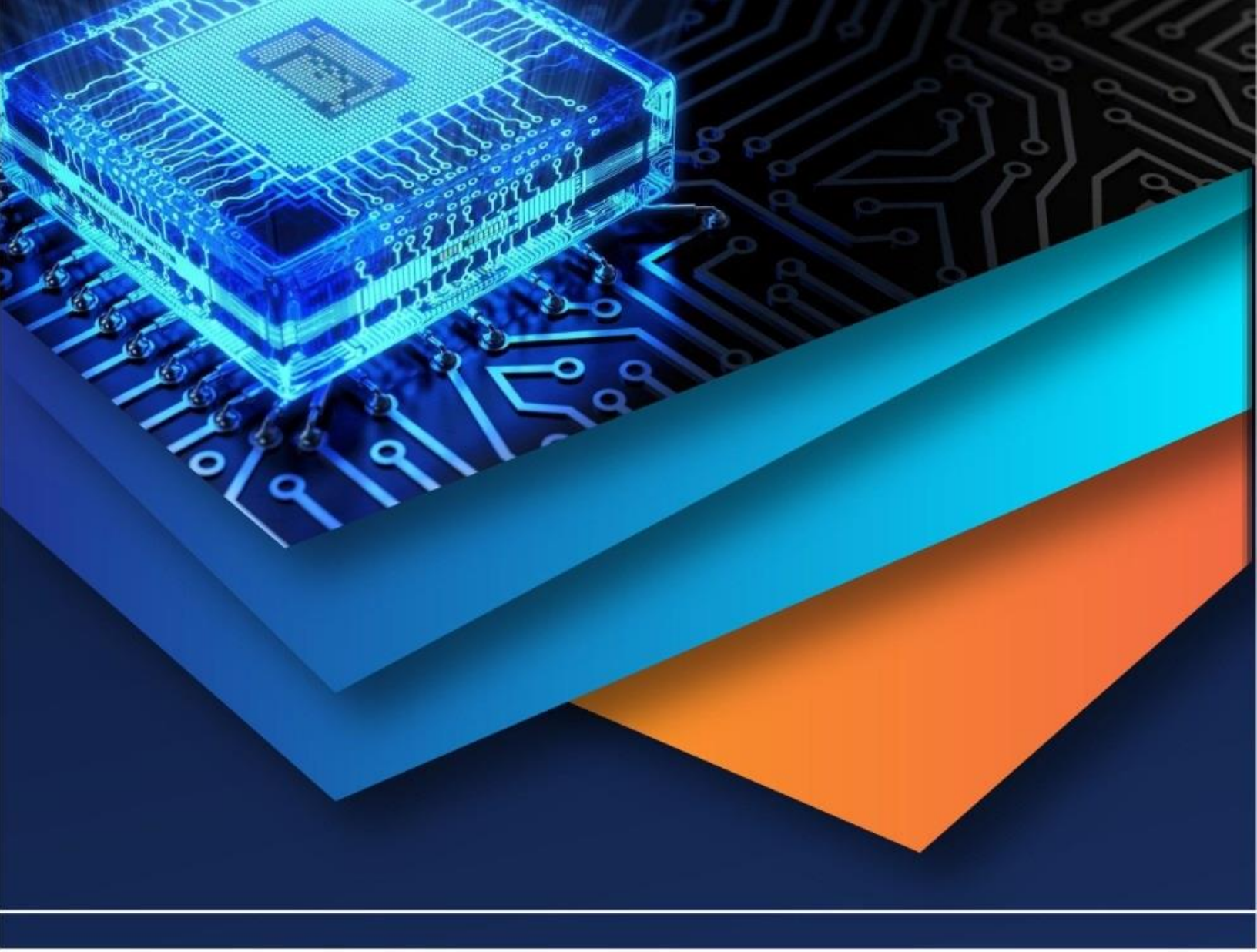

10.22214/IJRASET

45.98

IMPACT FACTOR: 7.129

IMPACT FACTOR: 7.429

INTERNATIONAL JOURNAL FOR RESEARCH

IN APPLIED SCIENCE & ENGINEERING TECHNOLOGY